Heliyon 9 (2023) e18760

Contents lists available at ScienceDirect

Heliyon

journal homepage: www.cell.com/heliyon

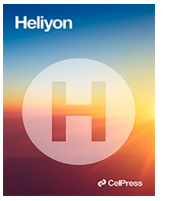

CO_2/CH_4 separation performance of SiO_2/PES composite membrane prepared by gas phase hydrolysis and grafting coating in gas-liquid membrane contactor: A comparative study

Zhengda Lin [a], Dandan Zhang [b], Yijun Liu [a], Zhongming Zhang [a], Zhiying Zhao [a], Bo Shao [a], Rui Wu [c], Rui Fang [d], Jie Yao [a,d,*]

[a] School of Environment, Harbin Institute of Technology, Harbin, 150090, PR China
[b] Harbin Institute of Technology Hospital, Harbin Institute of Technology, Harbin, 150090, PR China
[c] Guangdong Yuehai Water Investment Co., Ltd., Shenzhen, 518021, PR China
[d] Harbin Institute of Technology National Engineering Research Center of Urban Water Resources Co.,Ltd., No.73, Huanghe Road, Nangang Dist, Harbin, 150090, PR China

ARTICLE INFO

Keywords:
PES membrane
GLMC
Gas phase hydrolysis
Graft coating
SiO_2

ABSTRACT

The gas-liquid membrane contactor (GLMC) is a new and promising kind of gas separation technique, but still exhibits limitations, especially in membrane performance. In order to solve the above problems, we fabricated and characterized novel OH/SiO_2/PES composite membranes using gas phase hydrolysis and graft coating methods, respectively. In the preparation process, whether to use alkali to pretreat the membrane was used as an evaluation index. The CO_2/CH_4 separation performance was tested using the modified OH/SiO_2/PES hollow fiber membrane as the membrane contactor in GLMC. In the experiment, we conducted a single factor experiment with diethanolamine (DEA) as the adsorbent to analyze the effect of the flow rate and concentration of DEA on the separation of CO_2/CH_4. The collected gas had a CH_4 content of 99.92% and a CO_2 flux of 10.1059×10^{-3} mol m^{-2} s^{-1} while DEA at a concentration of 1 mol/L was flowing at a rate of 16 L/h. The highest separation factor occurred at this moment, which was 833.67. Overall, the CO_2/CH_4 separation performance in GLMC was enhanced with the use of the fluorinated OH/SiO_2/PES composite membrane.

1. Introduction

Given the situation of extreme global energy consumption, the current environmental pollution problem is becoming more and more serious [1]. A large amount of greenhouse gas emissions and energy waste caused by insufficient combustion of combustible gases have become major problems that need to be solved [2]. The traditional gas separation technology includes cryogenic method, air separation method and other methods [3–6]. The membrane separation method has a very good effect on gas separation. Through the shear force of the gas flow, the gas to be separated from the feed side passes through the membrane module by dissolution and diffusion to reach the permeate side of the membrane module in the traditional gas separation membrane [7]. In most gas separation, the performance of the membrane is represented by gas permeability and selectivity. There is a trade-off effect between membrane

* Corresponding author. School of Environment, Harbin Institute of Technology, Harbin, 150090, PR China
E-mail address: yaojiejiehit@163.com (J. Yao).

https://doi.org/10.1016/j.heliyon.2023.e18760
Received 29 June 2023; Received in revised form 25 July 2023; Accepted 26 July 2023
Available online 27 July 2023

permeability and selectivity. When the gas flux increases, the selectivity to the target substance will decrease. The decrease of gas separation membrane flux is a common problem of polymer membranes due to the increase of membrane age [8,9].

The development of GLMC offers an approach to overcome the challenge of low mass transfer efficiency and improve the overall effectiveness of the process [10]. The GLMC is a gas contact device used to remove CO_2. It is realized by an opposing flow of gas and liquid on both sides of the interface [11]. The hydrophobic microporous hollow fiber membrane is typically used as an interface barrier in gas-liquid contactors, where it can act as a carrier for the two phases while separating the liquid and gas phases. It allows for efficient mass transfer between the gas and liquid phases while preventing them from mixing [12]. Throughout the whole mass transfer process, the mixed gas passes through the hollow fiber membrane on its way from the gas phase side of the membrane surface to the liquid phase side under the effect of shear force. As a gas enters the liquid phase, it engages in a chemical reaction or physical absorption with the liquid absorbent [13]. The gas concentration on the liquid phase side is significantly reduced by the physical or chemical interaction between the liquid absorbent and the gas. With the flow of liquid absorbent and the continuous addition of new absorbents, the entire reaction system always maintains a certain mass transfer efficiency [14,15].

The main factor affecting the gas separation performance in the GLMC is wetting of the membranes [16]. One method to avoid membrane wetting is to use organic membranes with higher hydrophobicity [17]. However, the separation performance of a single hydrophobic organic membrane for CO_2 and the mechanical strength of the membrane itself cannot meet commercial requirements [18]. An effective way to overcome membrane wetting is to develop mixed matrix membranes (MMMs) [19]. Rosli fabricated and modified mixed-matrix membranes for CO_2 absorption. The modified mixed matrix membranes all showed better selectivity than the pristine membranes [20]. We maintain the mass transfer and separation efficiency of the gas-liquid membrane contactor by solving the membrane-wetting problem.

The concentration and type of absorbent have a significant impact on how effectively the gas is separated in the GLMC [21]. The membrane contactor serves as the gas-liquid interface for the complete reaction system [22]. When the absorbent is located on the liquid side, the physical and chemical reaction between the absorbent and the gas has a far greater impact on gas separation than the separation caused by the porosity and pore size of the membrane itself [23]. Hashemifard et al. prepared hollow fiber membrane contactor with polyvinyl chloride as raw material. The effects of calcium carbonate nanoparticles, relative humidity percentage of inlet air and gas-liquid flow rate on the surface modification of polydimethylsiloxane were investigated [24]. Mirfendereski used a membrane contactor to separate the mixture of CO_2 and H_2S under high gas-liquid ratio conditions. The experimental results showed that the membrane contactor can efficiently remove almost all H_2S in the case of large CO_2 content [25].

The basic unit of polyethersulfone (PES) is benzene ring, and the benzene rings are alternately connected by sulfur-oxygen double bonds and ether bonds [26]. Due to the stable chemical properties of the benzene ring, the chemical properties of PES are mild [27]. Since the upper and lower surfaces of the benzene ring form delocalized large π bonds, the presence of the upper and lower electron clouds protects the PES skeleton. Therefore, PES is resistant to high temperature and chemical corrosion [28]. PES is an asymmetric membrane, and the membrane pores are not absolutely uniform. The micropore diameter of the PES membrane is 100 Å, which is much larger than the diameter of the gas molecule, so the membrane has no screening effect on the mixed gas [29]. Based on the above characteristics, PES is suitable as a barrier between different phases in GLMC. However, the porosity of PES will lead to membrane wetting on the contact side between PES and liquid phase [30]. Therefore, the key to surpassing the gas separation efficiency of the membrane module is increasing the hydrophobicity of the membrane to address the wetting problem of the PES membrane. Surface modification or membrane blending are the two most common methods of membrane modification [31].

We devised and built a fluorinated SiO_2/PES composite membrane as a separation membrane in GLMC in this work. The membranes were prepared by the method of gas phase hydrolysis of silicon precursor and the method of graft coating, and then further hydrophobically modified. And whether the membrane is pretreated with alkali solution in the modification method was compared, and the influence of alkali treatment on the modification effect was analyzed. To explore the effects of DEA concentration and flow rate on CO_2/CH_4 separation, CO_2 flux and CO_2/CH_4 separation factor were used as separation performance indicators. Another component that was studied as part of the investigation was the mixed gas's flow rate.

2. Experimental

2.1. Materials

The original membranes were provided by Qingdao Donghai Membrane Co., Ltd. Sodium hydroxide (NaOH, 99 wt%), tetraethoxysilane (TEOS, 99 wt%), diethanolamine (DEA, ACS), tetraethoxysilane (TEOS),99.7 wt% isopropanol (IPA), diethanolamine (DEA, ACS) and ethanol (97%) were purchased from Wuhan Sevier Biotechnology Co., Ltd. 1H, 1H, 2H, 2H-perfluorodecyltriethoxysilane (PFTS, 99.7 wt%) was purchased from Chengdu Jinshan Chemical Reagent Co., Ltd.

We have purchased commercial PES hollow fiber membranes for surface modification. The 300 modified composite PES hollow fiber membranes were sealed as a group. A PVC membrane module was used to load PES composite membranes. The membrane module was sealed with polyurethane.

2.2. The method of membrane modification

The modification process of the novel gas phase hydrolysis method (GPHM) is as follows:

Firstly, the PES membrane was cleaned with deionized water and ethanol before being submerged in the NaOH solution (1 mol/L) at 70 °C. After that, the hollow fiber membrane was cleaned with deionized water and dried for 16 h in a hot oven at 60 °C.

Secondly, 1 g TEOS was fully dissolved with 1 g isopropanol to prepare TEOS isopropanol solution as (0.5 g/g). The TEOS solution was then combined with DEA to create a silicon precursor solution [32].

Thirdly, the pretreated and untreated PES hollow fiber membranes were soaked in the precursor solution at 60 °C as part of the grafting coating technique. The PES hollow fiber membranes, both pretreated and untreated, were immersed in a silicon precursor solution at a temperature of 50 °C to completely encapsulate the membrane surface with the silicon precursor solution. The membranes were then placed in an experimental box at a constant temperature and humidity of 100 °C for 30 min to hydrolyze the precursor. Out of the reaction container, the changed membrane was removed to cool naturally at ambient temperature. Following modification, the membrane was thoroughly rinsed with deionized water and dried for 12 h in an oven at 65 °C [15].

Finally, the produced composite membrane underwent hydrophobic fluorination modification. We prepared a 2 wt percent PFTS solution using ethanol as the solvent in order to dissolve the PFTS. To make it more consistent, the produced SiO_2/PES membranes were submerged in PFTS solution while being constantly agitated by the rotor. The membrane was pulled out and dried. Following drying, a sizable volume of ethanol and deionized water were used to wash the composite membrane. The composite membrane was then dried for 12 h in an oven set to 50 °C. Fig. 1 depicts a schematic representation of the OH/SiO_2/PES membrane modification method via the GPHM.

The modification steps of the PES membranes by traditional grafting coating method (GCM) and gas phase hydrolysis method were different, but the pretreatment and subsequent fluorination modification steps were exactly the same. After configuring the silicon precursor solution, we immersed the PES hollow fiber membranes in the silicon precursor solution. Then the water bath heating was used to control the temperature at 85 °C. Rotor stirring was used throughout the reaction to make the grafting uniform. The whole grafting process lasted for 12 h. After the modification was completed, the modified membranes were naturally cooled and placed in an oven to remove excess water and then fluoridated. The fluorination modification operation steps were exactly the same as those in GPHM. To verify the effectiveness of the approach we proposed, i.e., GPHM (gas-phase hydrolysis method), the traditional method GCM is utilized for comparison.

We have purchased commercial PES hollow fiber membranes for surface modification. The inner and outer diameters of the PES hollow fiber membrane were 0.8 mm and 1.4 mm, respectively. The total length and effective length of the membrane were 26 cm and 22 cm, respectively.

2.3. Membrane characterization

Energy dispersive X-ray spectroscopy (EDS) was used to determine the presence and distribution of novel elements (F and Si). SEM (ZEISS Sigma 500) was used to analyze the surface morphology of the membranes as well as the morphology of inorganic particles. The chemical linkages on the membrane surface were found using Fourier transform infrared (FTIR). The contact angle (CA) was used to detect the affinity between the membrane and the liquid phase. The structure and kind of SiO_2 crystal on the membrane surface were identified by XRD (X-ray diffraction). The bonding mechanism of the Si element on the surface of the sample and the chemical bindings of other elements were investigated using X-ray photoelectron spectroscopy (XPS). The roughness of the membranes was examined using atomic force microscopy (AFM). We listed the models and manufacturers of the required experimental instruments in Table 1.

2.4. Application of GLMC in CO_2/CH_4 separation

On the cavity side and shell side of the GLMC, respectively, gas and liquid flow in the experiment in the opposite directions. Table 2

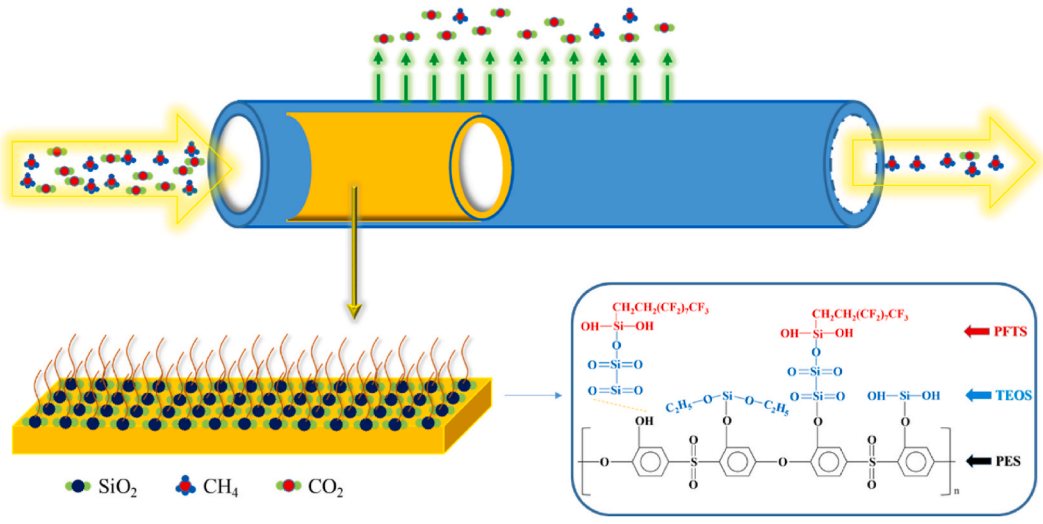

Fig. 1. Modification mechanism of PES membrane.

Table 1
Models and manufacturers of the required experimental instruments.

Type	Model	Manufacturer
Fourier transform infrared (FTIR)	Specturm100	Perkin Elmer, Inc.
X-ray diffraction (XRD)	X'PERT	Panalytical, Netherlands
Contact angle (CA)	JYSP-180	Beijing Jinshengxin Detection Instrument Co., Ltd.
SEM	S–3400 N	Hitachi, Japan
Energy dispersive X-ray spectroscopy (EDS)	Sigma-500	Hitachi, Japan
X-ray photoelectron spectroscopy (XPS)	ESCALAB 250Xi	Thermo Fisher, USA
atomic force microscopy (AFM)	Bioscope	American Vieco Company
Gas chromatograph (GC)	6890GC/7890 GC	Agilent Technology Co., Ltd.

displayed the membrane module's size specifications. Fig. 2 displayed the membrane module's schematic diagram. We supplemented the packaging process for these hollow fiber membranes. The 300 modified composite PES hollow fiber membranes were sealed as a group. A PVC membrane module was used to load PES composite membranes. The membrane module was sealed with polyurethane.

In order to imitate biogas, we used a CO_2/CH_4 mixed gas volume ratio of 40 : 60 for the experiment's starting gas. The explanation is that biogas has a CH_4 level of 55%–70% and a CO_2 content of 28%–44%. The CO_2 to CH_4 gas volume ratio is 40 : 60, which is consistent with the CO_2 and CH_4 gas concentration in biogas [33]. The duration of CO_2 absorption by the absorbent can be extended by the feed gas and absorbent flowing in the opposite directions [34]. As CO_2 may be absorbed by interacting with amine solutions, DEA is used as a CO_2 absorbent. The chemical molecule DEA, a secondary amine, may completely absorb and react with CO_2. As CH_4 and DEA do not interact, it remains on the gas side [31]. By single factor studies on DEA concentration, flow rate, and input gas flow rate, the ideal reaction conditions were identified. Gas chromatography was used to examine the CO_2 and CH_4 concentrations that were gathered at the gas outlet. In Fig. 3, the entire GLMC reaction cycle is shown.

The service life of the membrane is about 3 years. The maintenance requirements of the membrane: the membrane needs to be back washed with water for 5 min for 1 h. Periodic cleaning is required, and the general cleaning cycle is 1 week to 1 month. The specific situation depends on the operation of the membrane. The operation and maintenance cost of membrane: the labor cost, pharmaceutical cost and electricity cost of operation and maintenance are consumption costs. The cost of absorbent dosing and membrane replacement is a fixed consumption cost.

2.5. Calculation method

The profile is a schematic diagram of the membrane module, not the actual profile of the membrane module. The membrane module is a PVC material, which contains 300 PES composite hollow fiber membranes. We use polyurethane to seal the component to make it a complete kit. The equation is a consideration of the gas separation performance of the gas-liquid membrane contactor. The separation efficiency of CO_2/CH_4 was evaluated by separation factor. The larger the separation factor, the better the separation effect of gas-liquid membrane contactor on CO_2/CH_4. The CO_2 flux is used to directly characterize the amount of CO_2 passed through the membrane. These indexes jointly reflect the separation performance of gas-liquid membrane contactor for CO_2/CH_4 mixture.

CO_2 is absorbed by DEA through GLMC, and the calculation method refers to Equation (1) [14]:

$$J = \frac{P(Q_{in} - Q_{out})}{RTA_m} \tag{1}$$

where J is the CO_2 absorption flux (mol $m^{-2}s^{-1}$); Q is the gas flow of the feed gas ($10^{-3}m^3s^{-1}$); R is equal to a fixed value of 0.083 (bar L $mol^{-1}K^{-1}$); T is 298 K at room temperature; A_m is the effective surface area (m^2) of the PES membrane module, and P is the standard atmospheric pressure value of 1 bar.

The total pressure and static pressure of the fluid are measured by the total pressure tube and the static pressure tube respectively to determine the velocity of the fluid. How to use the specially designed composite pressure measuring tube to measure the total pressure and static pressure (or the difference between the two) of the fluid at the same time to determine the fluid velocity. When the total pressure pipe measuring the total pressure of the fluid is used, the axis of the pressure-sensitive hole should be aligned with the direction of the incoming flow. The difference between the total pressure and the static pressure of the liquid is directly measured by the pitot tube. With the increase of liquid flow rate, the difference between total pressure and static pressure increases. When the pressure difference reaches a certain value, the pressure generated by the liquid on the PES breaks through the upper limit of the pressure that the PES can withstand, resulting in membrane damage. The pressure at which the membrane is damaged is the liquid entry pressure (LEP).

The separation efficiency of the mixture is characterized by the CO_2/CH_4 separation factor. The value of CO_2/CH_4 separation factor

Table 2
Membrane module parameters.

Parameter	overall length (cm)	diameter (cm)	effective membrane length (cm)	total surface area (m^2)	effective specific surface area (m^2)
value	26	7	22	0.34	0.29

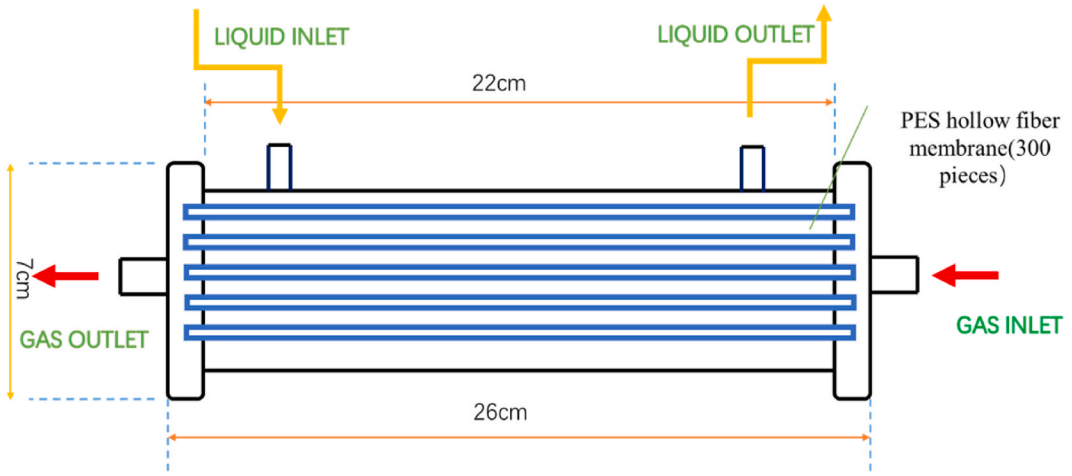

Fig. 2. GLMC reactor module.

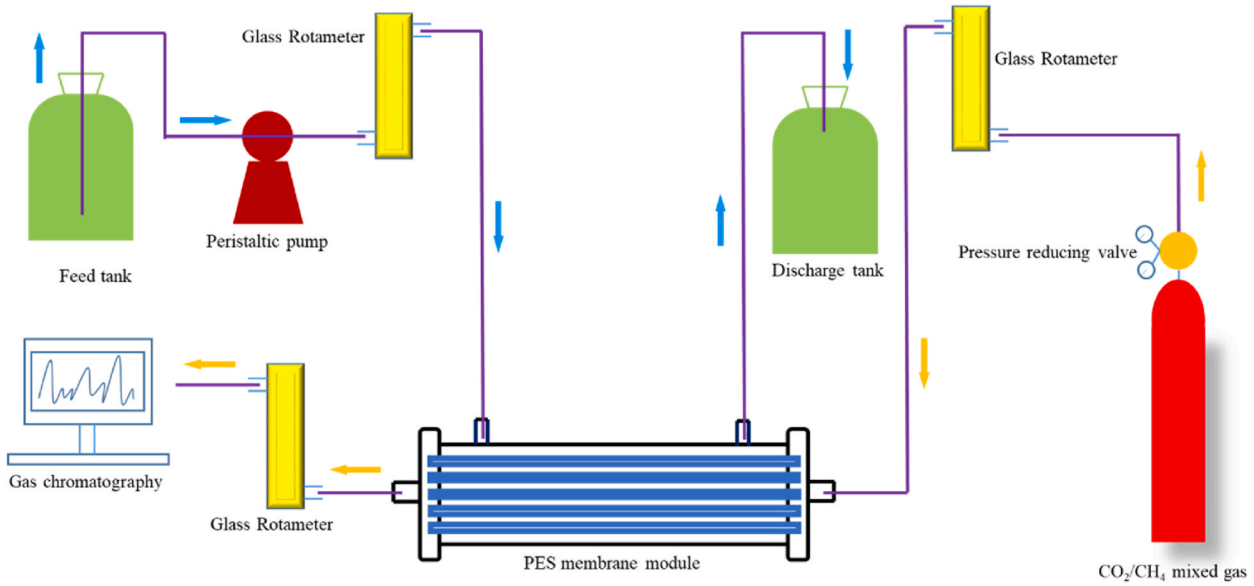

Fig. 3. Flow chart of GLMC for CO_2/CH_4 separation.

is calculated by equation (2) [35]:

$$\alpha = \frac{\frac{y_i}{y_j}}{\frac{x_i}{x_j}} \tag{2}$$

In the formula, x_i is the inlet side CH_4 concentration, x_j is the inlet side CO_2 concentration, y_i is the discharge side CH_4 concentration and y_j is the discharge side CO_2 concentration.

3. Results and discussion

3.1. Membrane characterization

We modified the PES membrane by gas phase hydrolysis and graft coating, respectively. At the same time, it is necessary to analyze whether the alkali treatment has an effect on the surface modification method. We labeled the original membrane and the membranes prepared by different modification methods with Roman numbers I, II, III, IV and V, respectively. The membranes represented by the corresponding serial numbers were listed in Table 3.

By using EDS analysis, it was possible to determine the elemental makeup and content of the PES membrane surface. Fig. 4 a showed that the conversion of TEOS and PFTS was successfully accomplished by the presence of Si and F components. The EDS values of different PES modified membranes were listed in Table 4. The distribution of the elements on the PES surface was uniformly revealed by the elemental fluorescence map, proving that TEOS and PFTS were grafted evenly. Meanwhile, the atomic mass fractions of F and Si elements are 28% and 13%, respectively. In Fig. 4 b, the surface Si content of the modified PES membranes increased sharply from 13% to 23.7%, while the corresponding F content decreased sharply from 13% to 4.8%. The atomic fluorescence images of Si and F elements indicated that their distribution was still uniform, proving that the grafting of TEOS and PFTS is still homogeneous in composite membranes made using the gas phase hydrolysis method (GPHM). In Fig. 4 c, the content of Si was further increased to 27.2%. The method of using high-temperature steam for the hydrolysis reaction has a higher conversion efficiency of TEOS to SiO_2 compared to the ordinary graft coating method (GCM) used on the PES membranes in Fig. 4 a. In Fig. 4 d, the content of Si was further increased to 32.3% and at the same time the content of F continued to decline. Compared with the membrane in Fig. 4 c, it can be concluded that the hydroxylated PES membrane was able to efficiently convert TEOS into SiO_2 in the hydrolysis reaction induced by high-temperature steam [36]. The reason is that after hydroxylation treatment, hydroxyl radicals can form anchor points on the benzene ring. The formation of anchor points can make the TEOS hydrolysis reaction proceed more smoothly. It is worth noting that as the content of the SiO_2 on the PES surface increase, the preparation method of the membrane tends to be superior. Hence, the content of the generation of the SiO_2, i.e., the grafting ratio of the SiO_2 on the surface of PES, indicates the effectiveness of the GPHM we proposed.

The mechanism of the reaction of silicon precursor solution to form SiO_2 by grafting coating method and gas phase hydrolysis method is different. The grafting coating method is to directly soak PES in the precursor solution of silicon for surface modification. The SiO_2 generated by the grafting coating method is attached to the surface of the PES substrate membrane and connected by hydrogen bond or van der Waals force. A large number of inorganic particles are generated, but there are not many inorganic particles that can directly form chemical bonds and crosslink on the membrane surface. After the hydroxylation treatment, a large number of hydroxyl sites cross-linked with the PES skeleton appeared on the membrane surface, so that the grafting coating reaction occurred at the hydroxylation site. Therefore, the generated SiO_2 is connected to the PES substrate by chemical bonds and is not attached to the surface. Therefore, for the graft coating method (GCM), the Si composition of SiO_2/PES decreased significantly after OH/SiO_2/PES. The gas phase hydrolysis method is to place the PES hollow fiber membrane with silicon precursor solution on the surface in a constant temperature and humidity box to undergo a dehydration condensation reaction with high-temperature water vapor to crosslink the generated SiO_2 on the surface of PES through chemical bonds. Because the hydrogen on the benzene ring of the PES skeleton is stable, the energy required for *C*–H cleavage is too high, so the amount of SiO_2 generated is less. However, after the hydroxylation treatment, a large number of hydroxyl anchors cross-linked with the PES skeleton appear on the membrane surface. The *O*–H in the hydroxyl groups connected to the benzene ring is very easy to break, so after the hydroxylation treatment, the increased number of anchors makes the PES surface connect more SiO_2. Therefore, for the gas phase hydrolysis method (GPHM), the Si composition of SiO_2/PES increased slightly after OH/SiO_2/PES.

SEM was used to describe the surface morphologies of the unaltered PES membrane and the modified membranes made using various techniques. The surface of the purified membrane was flat and smooth, as seen in Fig. 5 a. The surface of the hydroxylated PES membrane was covered with a significant number of regular wrinkles in Fig. 5 b. After hydroxylation treatment, it was found that the particle density generated on the surfaces of the prepared modified membranes depicted in Fig. 5 d and 5 f was higher than that of the membrane surfaces in Fig. 5 c and 5 e. This indicates that increasing the hydroxyl anchor sites on the PES surface can be accomplished by pretreating the membrane with hydroxyl before grafting. All of the modified membranes created as seen in Fig. 5 c and 5 d were created by the GCM. When Fig. 5 e and 5 f are compared, it is clear that although the grafting was not uniform, the density of the particles that developed on the surface was higher than that of the membranes created by the GPHM. After alkali treatment, the PES membrane's surface has more hydroxylation sites, and the hydrolysis of TEOS and hydroxyl groups on the PES surface results in the formation of more SiO_2 particles [37]. The PES membrane's surface particles after GPHM modification are comparatively uniform, and the particle distribution is obvious. The surface particles of the membranes are denser after the hydroxylation pretreatment.

In the FTIR spectra of all changed membranes in Fig. 6, the peak of the original membrane at 3304.68 cm^{-1} vanished. This shows that the *C*–H bond at 3304.68 cm^{-1} on the improved PES composite membrane surface vanishes. The skeleton of a benzene ring forms the foundation of the composite membrane, and the *C*–H bond that results from the sp^2 hybridization of the carbon atoms on the ring is broken. A new peak was seen at 2971.19 cm^{-1}, indicating that the broken *C*–H bond was replaced by the *C*–H stretching vibration on the aldehyde group [38]. The *C*–H bond is simultaneously broken and directly replaced by three chemical bonds, leading to the formation of three new *C*–H vibrations, as seen by the absence of the distinctive peaks of the benzene ring on the original membrane [39]. The benzene ring contains six coplanar carbon atoms, and each carbon atom forms three sp orbitals through sp^2 hybridization.

Table 3
Type of membrane.

serial number	Type of membrane
I	Pure PES membrane
II	SiO2/PES membrane (GCM)
III	SiO2/PES membrane (GPHM)
IV	OH/SiO2/PES membrane (GCM)
V	OH/SiO2/PES membrane (GPHM)

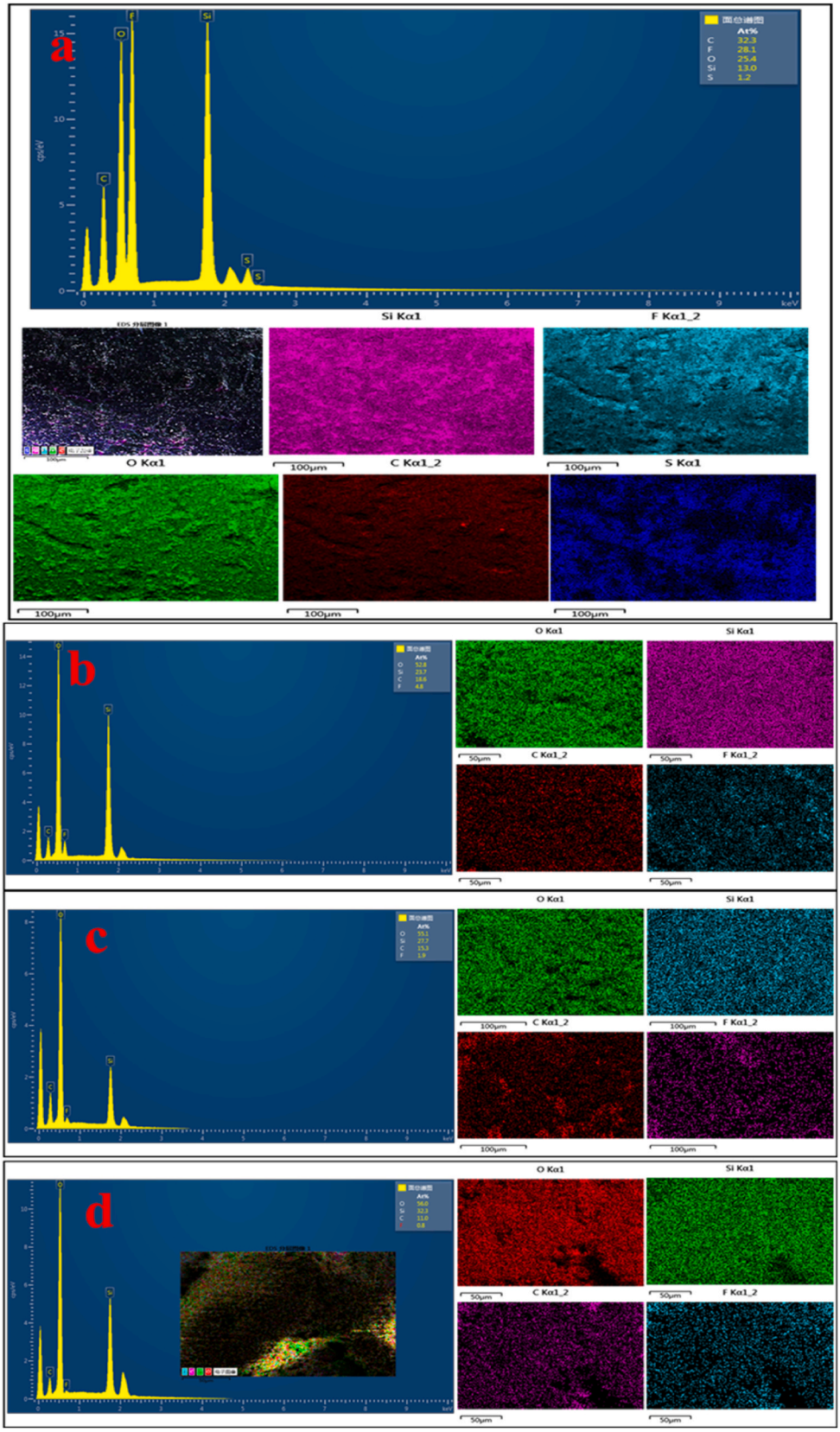

(caption on next page)

Fig. 4. EDS images of surface element composition and distribution of the PES membrane: (a) II; (b) IV; (c) III; (d) V.

Table 4
EDS values of different PES modified membranes (atomic percentage).

Types	C (%)	F (%)	O (%)	Si (%)	S (%)
II	32.3	28.1	25.4	13.0	1.2
IV	14.6	4.1	52.8	23.7	4.8
III	15.3	1.9	55.1	27.7	0.5
V	11.0	0.3	56.0	32.3	0.4

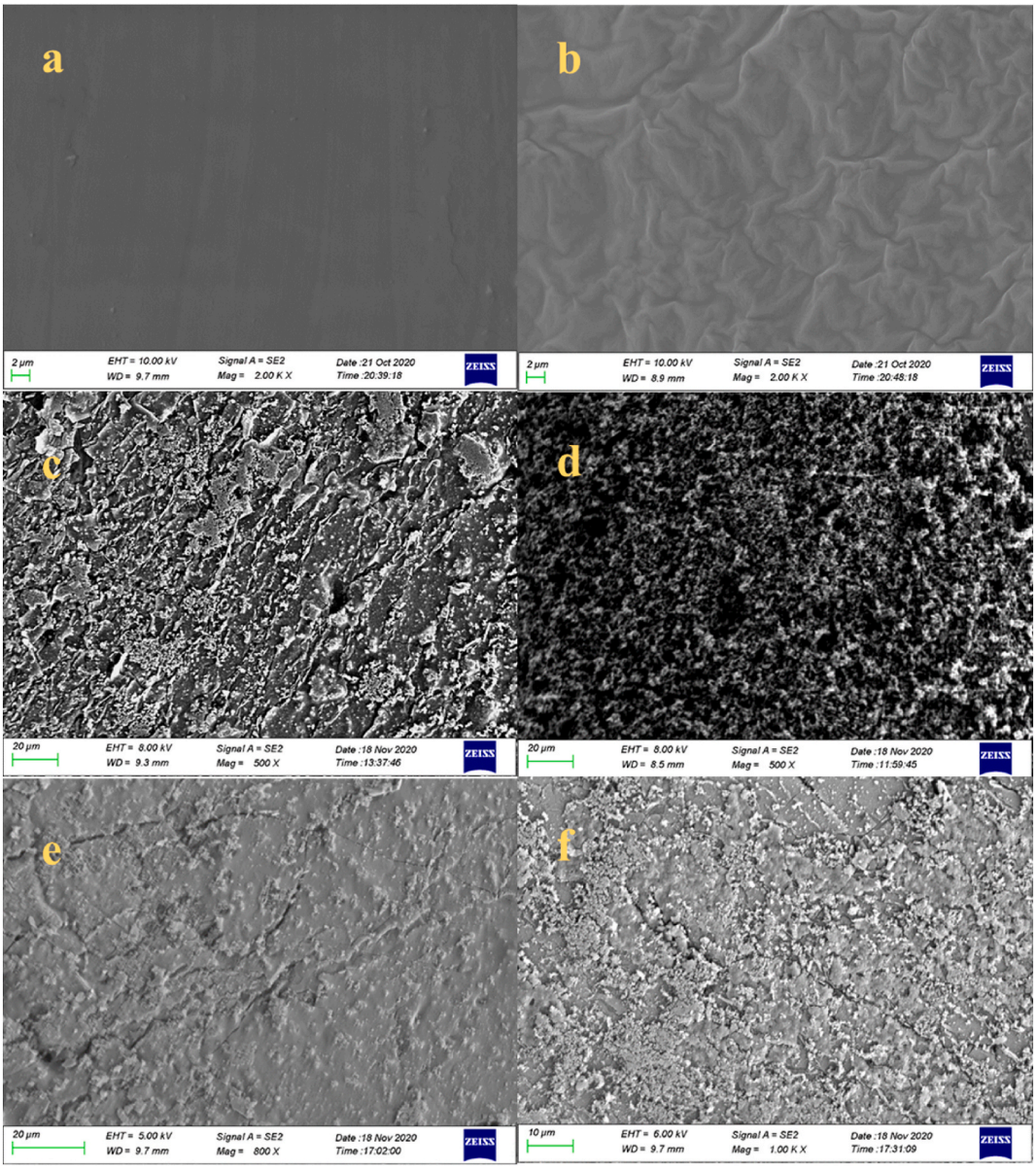

Fig. 5. SEM of PES membrane: (a) I; (b) the pretreatment of PES membrane surface with NaOH; (c) II; (d) IV; (e) III; (f) V.

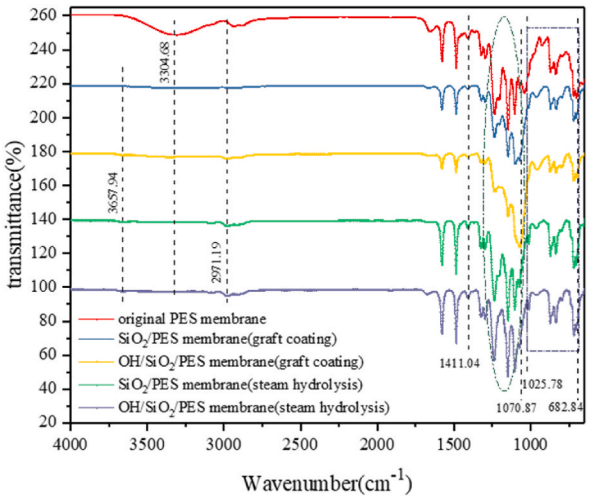

Fig. 6. FTIR spectra of the PES membranes.

One sp orbital on each carbon atom overlaps each other to form a *C*–C bond, and six high-energy σ bonds form six *C*–C bonds, forming the basic skeleton structure of the benzene ring. Two opposing C atoms occupy one sp orbital, connected to the sulfur and oxygen atoms, respectively. The remaining four carbon atoms occupy one sp orbital respectively and are connected with hydrogen atoms to form *C*–H bonds. Each of the six carbon atoms leaves one sp orbital distributed on the same side of the benzene ring, and the electron clouds overlap each other, forming a large delocalized π bond in the ring structure. The above chemical bonds work together to form the basic framework of PES. A characteristic peak of carbon atoms at 1411.04 cm^{-1} on the benzene ring was detected on the modified membrane, indicating that the π bond still exists. The replacement of the *C*–H bond by the *C*–Si bond, with a very strong variable angle vibration, was shown by the new peak at 1025.78 cm^{-1}. The presence of the *C*–Si bond indicates that the grafting of TEOS onto the benzene ring of PES was effective [40]. The emergence of the new peak at 1070.87 cm^{-1} indicated the presence of variable angle vibration in the synthesized *C*–*O*–Si bond [36]. A new peak at 3657.94 cm^{-1} indicated the formation of hydrogen bonds stronger than van der Waals force. There were several absorption peaks in the benzene ring's fingerprint area that collectively make up the ring. The benzene ring-to-benzene ring bond is represented by the box section as the fingerprint region. The benzene ring in the PES skeleton is connected by ether bond or sulfone or sulfoxide. The fingerprint region of the box represents the structure of the polyethersulfone [37]. The modified composite membrane's fingerprint region matched the original membrane's perfectly, proving that the benzene ring skeleton on the modified polyethersulfone did not alter. The aforementioned findings showed that the base membrane did not alter and that the modification was made to the original membrane's surface. The FTIR characteristic bands of all the PES membranes were summarized in Table 5.

We added SiO_2 to the PES membrane surface and then further fluorinated it to enhance the composite membrane's hydrophobicity which can be immediately determined by the contact angle. The contact angle of the PES membrane after alkali treatment dropped from 94° to 97.1°–86° to 89°, as shown in Fig. 7 a and 7 b. This shows that the PES membrane's initial hydrophobicity was not very powerful, and that its contact angle after being exposed to alkali shrank and even exhibited a hint of hydrophilia. The reduction in CA demonstrated that, following alkali treatment, hydroxyl radicals were effectively crosslinked onto the PES [41].

Fig. 7 c, 7 d, 7 e, and 7 f show that the contact angles of SiO_2/PES membranes produced by GCM and GPHM with and without alkali treatment were 134°, 142.7°, 108.8°, and 124.6°, respectively. After alkali treatment of PES membrane, hydroxyl radicals are fixed on the PES membrane base layer, so that TEOS can react with HO· on the benzene ring to increase the hydrolysis amount [42]. During the hydrolysis process, the σ bond of the hydroxyl radical immobilized on the PES skeleton breaks to generate free radical H, which provides the redox potential. The free radicals undergo electron transfer with the active groups in TEOS to form SiO_2 connected to the surface of PES [43].

According to the techniques of production, the PES composite membrane created by GCM has a higher hydrophobicity. The purpose of GCM is to bring the membranes into touch with the TEOS solution, increasing the volume of material that comes into

Table 5
FTIR characteristic bands of all the PES membranes.

Wavenumber (cm^{-1})	3304.68	2971.19	1411.04	1025.78	1070.87	3657.94	fingerprint region
I	✓	–	✓	–	–	–	✓
II	–	✓	✓	✓	–	✓	✓
IV	–	✓	✓	✓	✓	✓	✓
III	–	✓	✓	✓	–	✓	✓
V	–	✓	✓	✓	✓	✓	✓

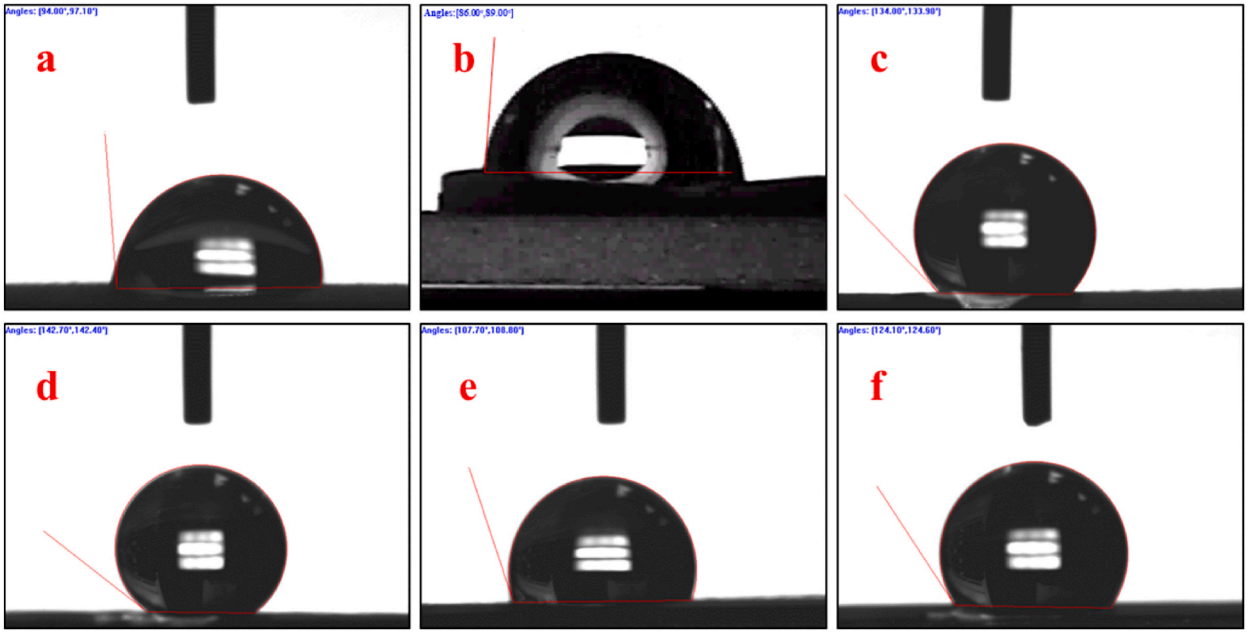

Fig. 7. Water contact angle (WCA): (a) I; (b) the pretreatment of PES membrane surface with NaOH; (c) II; (d) IV; (e) III; (f) V.

contact with water molecules and TEOS. PES and TEOS are encircled by water mist rather than liquid water when using GPHM, and TEOS has a reduced contact area [37].

In summary, although the hydrophobicity of PES decreased slightly after alkali treatment, the increased ·OH will be combined with more SiO_2 hydrolyzed by TEOS. The hydrophobicity of the hybrid membrane was further enhanced by the addition of PFTS. By increasing its hydrophobicity, the composite membrane will have less time in touch with liquids, making it more appropriate for use as a gas-liquid separation barrier in GLMC [39].

There is a correlation between surface roughness and water contact angle. The greater the surface roughness, the greater the value of the water contact angle. We prepared PES composite membranes by surface modification of PES. A large number of SiO_2 particles are attached to the surface of the composite membrane. The surface roughness of the composite membrane can be obtained by AFM and SEM. The value of the water contact angle is directly measured by the contact angle meter. Through experimental analysis, we conclude that there is a correlation between surface roughness and water contact angle.

The strength of the membrane is a necessary indicator of whether the membrane can be produced on a large scale. The physical properties of the membranes were characterized by measuring the stretched length and elongation of the membranes using a stretching machine [41]. The physical properties of the membranes were listed in Table 6. The breaking strength and the elongation rate of the SiO_2/PES membranes unhydroxylated by graft coating increased about 9.1% and 4% more than original PES membranes, respectively. The breaking strength and the elongation rate of the OH/SiO_2/PES membranes by graft coating increased about 15.7% and 5.7% compared to the pristine membranes, respectively. The breaking strength and the elongation rate of the SiO_2/PES membrane undroxylated by the GPHM increased about 5.8% and 7.3% more than the original membranes, respectively. The breaking strength and the elongation rate of the OH/SiO_2/PES membrane by the GPHM increased about 12.4% and 8.9% compared to the original membranes, respectively [44].

The mechanical strength of the SiO_2/PES membranes had improved to some degree, as evidenced by the greater breaking strength and elongation of the modified membrane. However, the modified membrane's water flux did marginally reduce. Additionally, the hydroxylation-pretreated membrane's water flow dropped even more. The modified PES membranes had a substantial quantity of SiO_2 adhered to their surface, which interfered with the unrestricted movement of water molecules into and out of the membrane pores. As a result, the composite PES membranes' water flow had been somewhat decreased. More TEOS was hydrolyzed, attached to the hydroxyl anchors on the PES surface, and mixed on the surface following the hydroxylation preparation. As a result, the modified PES

Table 6
Physical properties of membranes.

Parameter	I	II	IV	III	V
Breaking strength(N)	121 ± 1.414	132 ± 1.549	140 ± 2.449	128 ± 2.000	136 ± 1.673
Elongation (%)	123 ± 2.324	128 ± 2.098	130 ± 2.191	132 ± 1.414	134 ± 2.646
Water flux under 50 kPa (kg $m^{-2}h^{-1}$)	19 ± 0.632	15 ± 1.095	13 ± 1.673	16 ± 0.632	12 ± 0.632
Water flux under 100 kPa (kg $m^{-2}h^{-1}$)	28 ± 1.673	21 ± 0.632	19 ± 1.095	20 ± 1.095	18 ± 0.632

membranes with hydroxylation prior to modification had a reduced water flow than the modified membrane without hydroxylation.

The above results showed that the physical and mechanical properties of the modified PES membranes were superior to those of the pristine PES membranes.

Fig. 8 showed the roughness of the membranes and the arithmetic mean and square mean of the surface roughness were recorded in Table 7. Ra was 36.8 nm, and Fig. 8 a demonstrated that the initial PES membrane's surface was smooth. The R_a are 156 nm and 103 nm, respectively, in the AFM pictures of the SiO_2/PES composite membrane and the OH/SiO_2/PES composite membrane created by GCM. In Fig. 8 b and c, the AFM images of the SiO_2/PES composite membrane and the OH/SiO_2/PES composite membrane produced by GCM shows the corresponding R_a values were 156 and 103 nm, respectively. Fig. 8 d and 8 e, respectively, show the AFM images of the SiO_2/PES composite membrane and the OH/SiO_2/PES composite membrane produced by GPHM. The corresponding R_a values were 193 and 127 nm.

Regardless of the alteration technique used, the modified PES membrane treated with hydroxylation has less surface irregularity than the modified PES membrane not treated with hydroxylation. The benzene ring skeleton of PES is linked to a significant quantity of hydroxylation produced by alkali treatment. The breakdown of TEOS benefits from the hydroxylation spots on the benzene ring. Thus, membrane change following alkali therapy will result in the production of more SiO_2. Additionally, the GPHM-modified membrane has a rougher surface than the GCM-modified membrane. Water molecules in vapor form are pyrolyzed to create hydroxyl radicals during the GPHM hydrolysis process. Therefore, TEOS can interact with additional hydroxyl groups. TEOS and liquid water come into touch with each other and react on the surface of the PES membrane during the GCM modification process. In conclusion, GPHM is a superior modification technique than GCM [37].

XRD was used to identify the appearance of SiO_2 on the membrane surface. As illustrated in Fig. 9, the GPHM or the GCM can identify the SiO_2 (PDF: 82–1564) diffraction peaks on the modified PES membranes. The (0 0 1) and (1 0 0) crystal planes of SiO_2 crystal can be found by comparing XRD images with PDF cards of SiO_2 [36,40].

The diffraction peak intensities of SiO_2 crystals detected on the surface of hydroxylated membranes were higher than those of unhydroxylated membranes regardless of whether the PES membranes were modified by GPHM or GCM. This indicates that the hydroxylation treatment can increase the modified grafting rate and make the surface generate more SiO_2.

There are two purposes of the modification: (1) Increasing the hydrophobicity of the composite membrane, thereby reducing the mass transfer resistance of the absorbent and the membrane. (2) The surface modification of PES makes the substrate membrane wrapped by inorganic material (SiO_2), thereby reducing the damage of alkaline absorbent to the PES substrate membrane.

Using XRD to detect the crystallinity of the composite membrane is a joint proof of FTIR and XPS characterization of the surface functional groups of the composite membrane. These characterizations publicly prove the successful formation of SiO_2 and its grafting onto the surface of PES. The successful preparation of the composite membrane not only increases the hydrophobicity of the membrane and improves the separation performance of the membrane in the gas-liquid membrane contactor, but also reduces the corrosion effect of the alkaline absorbent on the membrane, prolongs the service life of the membrane, and increases the acid and alkali resistance of the membrane.

The Le Chatelier principle states that as reactant concentration rises, product concentration will follow. The amount of TEOS and

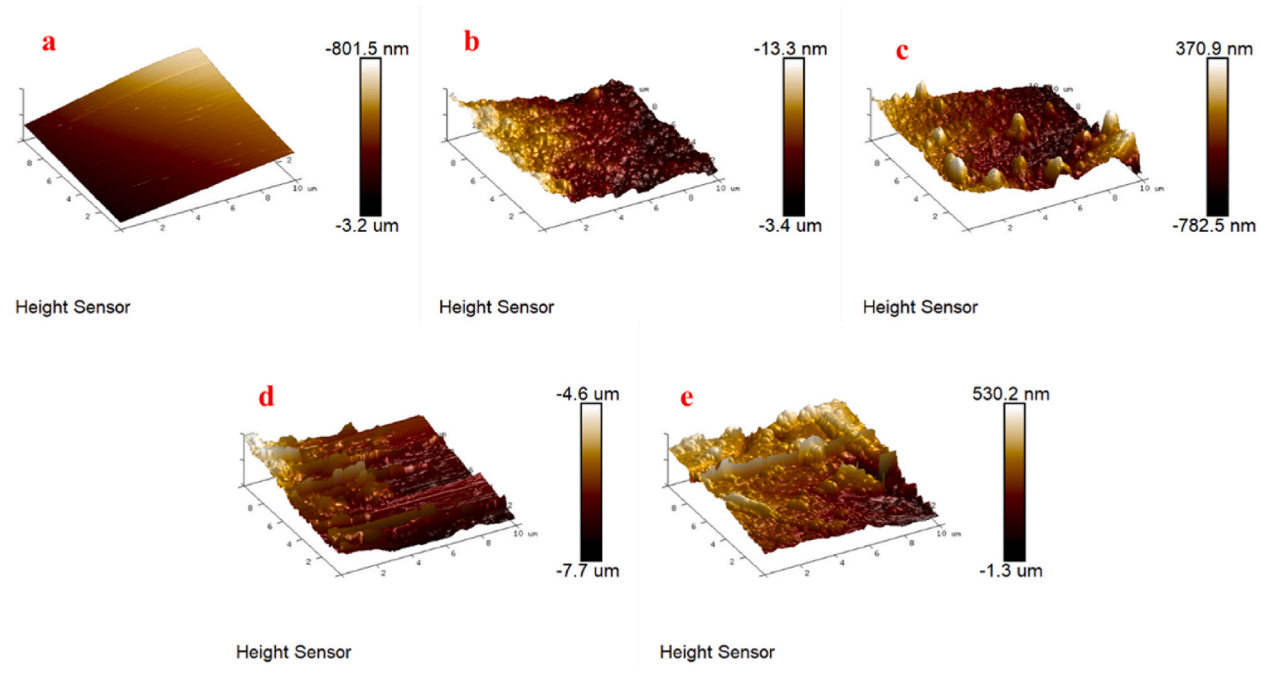

Fig. 8. AFM images of the PES membranes: (a) I; (b) II; (c) IV; (d) III; (e) V.

Table 7
Surface roughness parameters of PES membranes.

Sample	a	b	c	d	e
Ra[a](nm)	36.8	156	103	193	127
Rq[b](nm)	48.8	242	141	247	173

[a] R_a: the arithmetic mean of roughness.
[b] R_q: the mean square root of roughness.

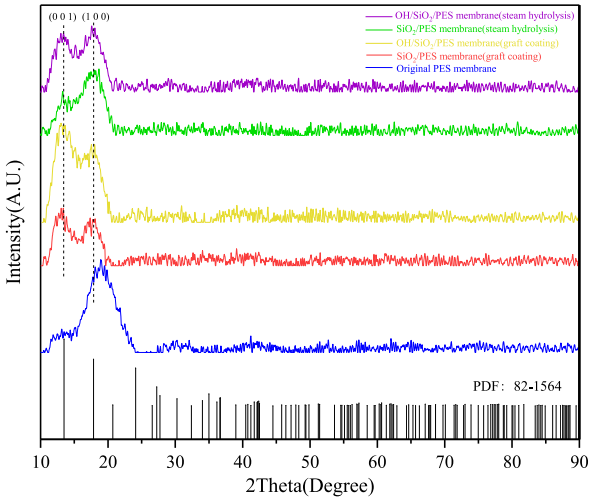

Fig. 9. XRD patterns of the membranes.

water vapor retained on the surface of GPHM during the preparation process is used as the reactant to determine the amount of SiO_2 produced by the less content of TEOS. During the modification process of GCM, PES was immersed in TEOS solution, so there was a sufficient supply of reactants. As a result, the composite membrane created by GCM has a larger SiO_2 concentration than the membrane prepared by GPHM. The condition of the reactants distinguishes GPHM from GCM. In the GPHM, TEOS is employed to interact with gas phase water, whereas in the GCM, TEOS reacts with liquid phase water. The SiO_2 uniformity of the membranes created by GPHM can be better than those that prepared by GCM because the gaseous reactant can carry out the reaction more thoroughly than the liquid reactant.

The chemical bonding of the elements on the membrane surface may be successfully analyzed using XPS, and Table 8 recorded the atomic concentration of each element. The XPS spectra of the membranes produced by the GCM with and without hydroxylation treatment are shown in Fig. 10 a_1 and b_1, respectively. The XPS spectra of unhydroxylated and hydroxylated PES composite membranes made by the GPHM, respectively, were displayed in Fig. 10 c_1 and 10 d_1. The original membrane's XPS spectra was shown in Fig. 10 e_1.

The XPS spectra of PES composite membranes made using the two procedures showed the typical peaks of silicon atom with Si 2p binding energy of 103.08 eV and fluorine atom with F 1s binding energy of 689.08 eV [45]. The *Si*–C bond, the O═Si═O link, and the SiO_x bond created three sub-peaks on the 2p orbital in the XPS spectrum, with binding energies of 102.77 eV, 104.08 eV, and 105.08 eV, respectively. The XPS spectra of Si in Fig. 10 a_2, b_2, c_2, d_2 and e_2 showed that Si atoms directly form SiO_2 chemical bonds on the 2p orbital and also directly form SiO_2 crystals.

The binding energies for the individual components of the overall peak of C 1s in Fig. 10 a_3 are as follows: The new peaks of CF_3, CF_2 and *C*–F at 293.15 eV, 290.88 eV and 288.15 eV, respectively, confirmed that F element was successfully connected to PES. The presence of carbides at 286.62 eV (*C*–*O*–C), 285.68 eV (285.68 eV) and 284.09 eV indicated the integrity of PES. In the C 1s XPS spectra of Fig. 10 b_3, the positions of the *C*–C, CF_3, *O*–C═O and CF_2 bonds were 284.8 eV, 293.75 eV, 288.74 eV, and 291.43 eV, respectively.

Table 8
Elemental composition (atomic percentage).

	F 1s (%)	O 1s (%)	C 1s (%)	S 2p (%)	Si 2p (%)
II	22.74	34.15	27.42	0.03	15.63
IV	52.38	32.28	10.46	0.24	4.65
III	32.77	51.06	9.16	_	7.02
V	28.61	54.42	9.84	_	7.14
I	_	42.64	51.37	5.27	_

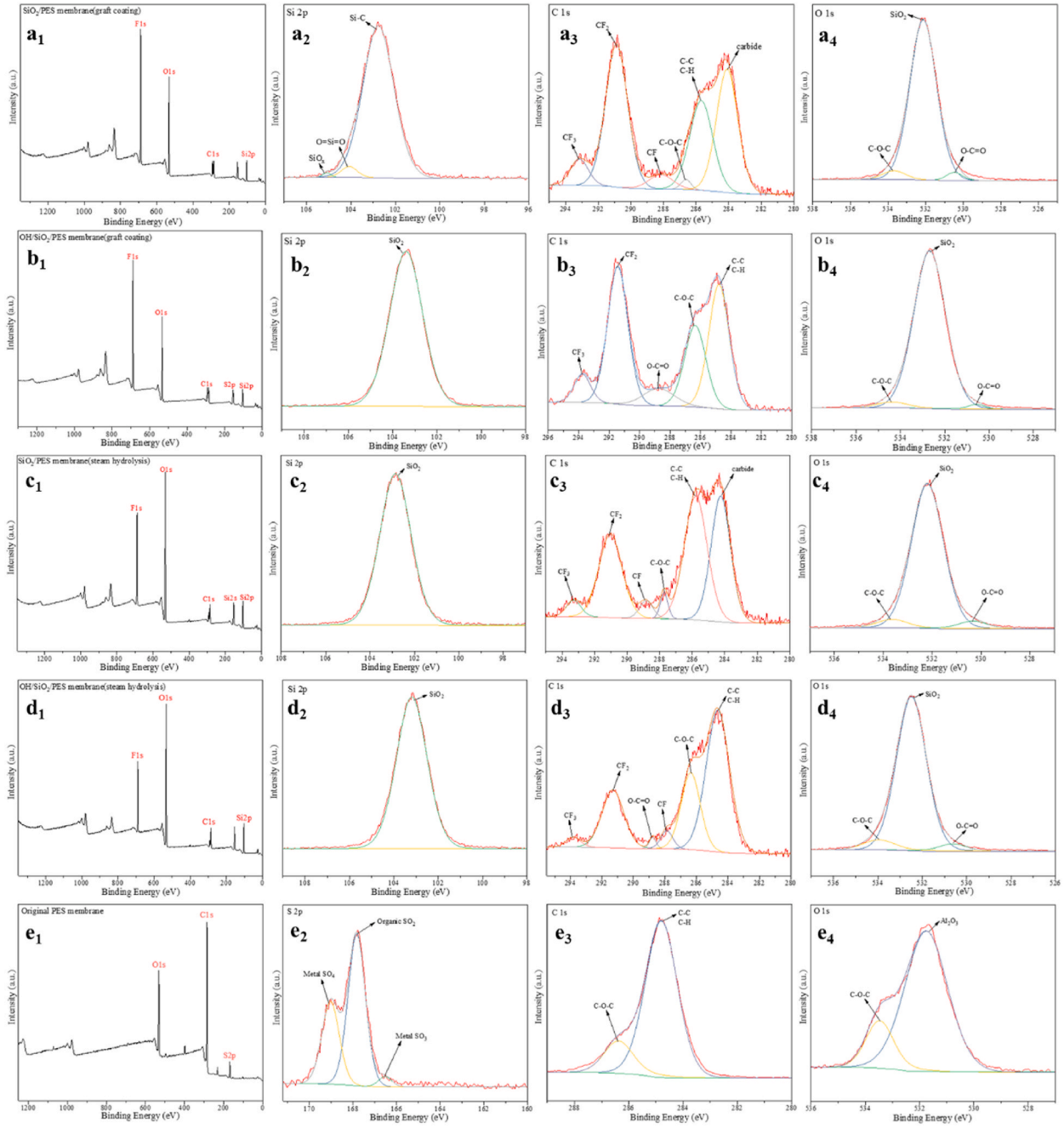

Fig. 10. XPS spectra of (a_1) XPS survey scan spectra, (a_2) Si 2p, (a_3) C 1s, (a_4) O 1s on II; XPS spectra of (b_1) XPS survey scan spectra, (b_2) Si 2p, (b_3) C 1s, (b_4) O 1s on IV; XPS spectra of (c_1) XPS survey scan spectra, (c_2) Si 2p, (c_3) C 1s, (c_4) O 1s on III; XPS spectra of (d_1) XPS survey scan spectra, (d_2) Si 2p, (d_3) C 1s, (d_4) O 1s on V; XPS spectra of (e_1) XPS survey scan spectra, (e_2) S 2p, (e_3) C 1s, (e_4) O 1s on I.

Fig. 10 c_3 and Fig. 10 d_3 showed the number and location of C 1s sub-peaks on the membranes prepared by GPHM. The kinds and binding energies of the C 1s peaks of the composite membranes created by GCM were the same as the peak fitting results for the overall C peak. The original PES membrane of C 1s sub-peaks is shown in Fig. 10 e_3. The membranes created by GPHM and GCM had three sub-peaks of O 1s, and Fig. 10 a_4, b_4, c_4, and d_4 revealed that they were *C–O–*C (534.38 eV), O═Si═O (532.68 eV), and *O–*C═O. (530.58 eV). The original PES membrane of O 1s sub-peaks is shown in Fig. 10 e_4. The presence of O═Si═O detected in the sub-peak of the oxygen element is the same as the result of SiO_2 detected in the XPS peak separation of the silicon element. At the same time, the oxygen atom is hybridized in the 1s orbital, and the silicon is hybridized in the 2p orbital. Therefore, it can be concluded that the two p orbitals of the silicon element overlap with the s orbitals of the two oxygen atoms after hybridization to form two sp hybrid orbitals.

The orbital hybridization theory is consistent with the detected O═Si═O results [46].

3.2. Measurement of CO_2/CH_4 separation performance in GLMC

It can be seen from the characterization of the SiO_2/PES composite membrane described above, as well as from an analysis of the results, that alkali treatment of the base membranes can increase the number of hydroxyl group anchor points, as well as the concentration of hydrolysis and crosslinking between the base membranes and the SiO_2 crystals. The membranes created by GPHM have greater SiO_2 crystal density and homogeneity than those prepared by GCM, according to the findings of the characterization. This section assessed the SiO_2/PES composite membranes' ability to separate gases and examined the influence of various preparation techniques on the performance of the composite membranes. As the primary element of the gas-liquid membrane contactor, the SiO_2/PES composite membrane manufactured using the best preparation technique was chosen. In order to trap CO_2 in GLMC, we utilized DEA as an absorbent [10]. CH_4 remains on the gas phase side and is ejected from the collecting port in the airflow direction [47].

3.2.1. Comparison of separation performance of GPHM and GCM modified membranes

We assessed the mixed gas separation capabilities of the PES membranes and investigated the impacts of various modification techniques on the CO_2 flow and CO_2/CH_4 separation factor of multifunctional composite membrane materials in order to replicate the gas separation performance of membrane materials under real-world settings. GCM and GPHM, respectively, created PES composite membranes. The hydroxylation alkali treatment was used to create the composite membranes created by each alteration procedure. Fig. 11 depicts the outcomes of CO_2/CH_4 separation using various membranes.

The volume percentage of CO_2 and CH_4 on the collecting side provides an intuitive way to determine the purity of the collected gas (Fig. 11 a). At the collecting side of the original membrane, the volume percentage of CO_2 is 5.4%, which corresponds to the volume fraction of CH_4 at 94.6%. On the collecting side of the membrane created by GCM, the volume percentage of CO_2 was 1.5% and the volume fraction of CH_4 was 98.5%. On the collecting side of the SiO_2/PES membrane created by GPHM, the volume proportion of CO_2 was 1.3%, practically identical to that of the composite membrane created by GCM, while the volume fraction of CH_4 was 98.7%. After alkali treatment, the volume percentage of CO_2 on the collecting side of the OH/SiO_2/PES membrane prepared by GCM was 0.8%, while that of CH_4 was 99.2%. The separation effect has been enhanced much further. After alkali treatment, the corresponding volume percentages of CO_2 and CH_4 on the collecting side of the OH/SiO_2/PES membrane modified by GCM were 0.5% and 99.5%, respectively. It can be shown that the modified membrane collects CH_4 with a higher degree of purity than the pure PES membrane. The separation performance of the membrane was further characterized in Fig. 11 b by the CO_2 flux and CO_2/CH_4 separation factor. The CO_2/CH_4 separation factor rose from 11.68 of the original membrane to 43.78 of the membrane created by the GCM and 50.62 of the membrane prepared by the GPHM due to the modified membranes' higher CO_2 fluxes. In comparison to the original membrane, which had a separation factor of 82.67 and 132.67, the composite membrane changed by alkali treatment and further modified by GCM and GPHM had a higher separation factor. The separation performance of the membranes made by GPHM was superior than that of membrane made by GCM under the same pretreatment, according to comparisons of II with III, IV, and V. That SiO_2 is distributed more uniformly and is more tightly bound to the PES surface which improves separation performance. Considering the findings of II and IV, III and V, it can be said that alkali treatment results in a significant number of hydroxylated connection sites being connected to the surface of PES regardless of the modification technique utilized.

Given the aforementioned findings, it can be inferred that alkali treatment followed by surface modification can enhance the composite membrane's separation capabilities. Second, the separation effect of the membranes produced by GPHM and GCM is superior to that of the original membrane, and GPHM is a superior approach to GCM for surface modification.

We compared the parameters of the OH/SiO_2/PES composite membrane with the original PES membrane, as shown in Table 9. The liquid breakthrough pressure test was performed to characterize the mechanical properties of the membranes. The liquid entry pressure (LEP) of the original membrane was 0.2 MPa, and the liquid entry pressure (LEP) of the modified membrane was 0.3 MPa. The

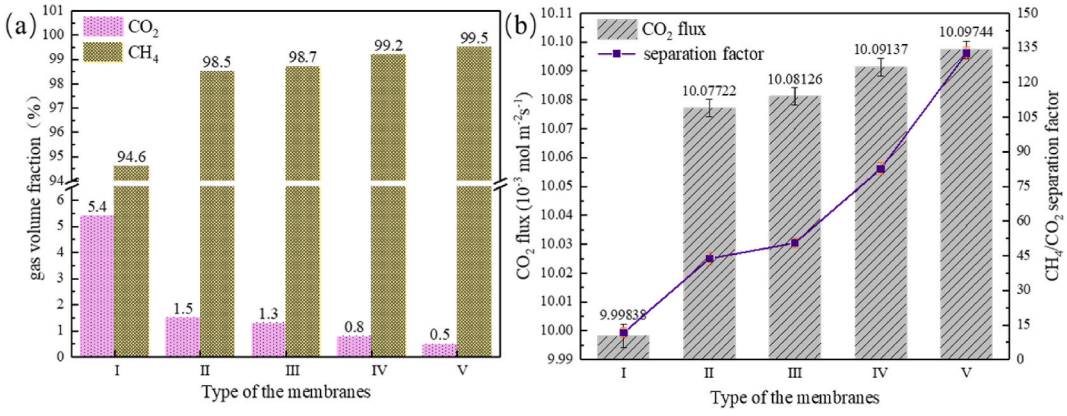

Fig. 11. Separation performance of pure PES membrane and various modified PES composite membranes.

Table 9
Membrane parameters.

Parameter	Original PES membrane	OH/SiO_2/PES membrane
Inner diameter (mm)	0.8	0.8
Outside diameter (mm)	1.4	1.4
Alcohol Bubble Point (MPa)	0.48	0.53
Liquid entry pressure (MPa)	0.2	0.3
pure water flux (L/(m^2 h))	75	68
molecular weight cut-off (Dalton)	10,000	16,000
Average pore size (μm)	0.1	0.1
Porosity	60%	60%

liquid entry pressure (LEP) indicates the difficulty of membrane wetting. The smaller the LEP value, the smaller the flux. Excessive LEP will lead to excessive breakthrough pressure and membrane damage.

3.2.2. *The influence of external factors on the separation performance of CO_2/CH_4*

We select OH/SiO_2/PES composite membrane in GLMC because the membrane has the best gas separation performance when created by the GPHM following hydroxylation. The CO_2 flux in the collected gas and the CO_2/CH_4 separation factor serve to identify the mixed gas's separation effectiveness. In Fig. 12 a and b, DEA solution with a concentration of 1 mol/L was employed as the absorbent under the conditions of a gas flow rate of 60 ml/min, and the separation efficiency of CO_2/CH_4 was addressed using the absorbent flow rate as an influencing factor. The pure PES membrane's CO_2 concentration was 30.5%, its CO_2 flux was 9.49×10^{-3} mol m^{-2} s^{-1}, and its CO_2/CH_4 separation factor was 1.52 at a DEA flow rate of 1.6 L/h. The CO_2/CH_4 separation factor was 2.38 in accordance with the CO_2 concentration of the OH/SiO_2/PES membrane, which was 21.9%, CO_2 flux of 9.66×10^{-3} mol m^{-2} s^{-1}. When the DEA flow rate was 3 L/h, the CO_2 flux was 9.65×10^{-3} mol m^{-2} s^{-1}, the CO_2 concentration of pure PES membrane was 22.4%, and the corresponding CO_2/CH_4 separation factor was 2.31. The OH/SiO_2/PES membrane had a CO_2 concentration of 16.6%, a CO_2 flow of 9.77×10^{-3} mol m^{-2} s^{-1}, and a CO_2/CH_4 separation factor of 3.35 at this point. Pure PES membrane and modified composite membrane have very little separation performance difference when the absorbent flow rate is modest. The efficiency of separation is not significantly affected by an increase in absorbent flow rate. The CO_2 concentration of the pure PES membrane was 2.2%, the CO_2 flux was 10.06×10^{-3} mol m^{-2} s^{-1}, and the corresponding CO_2/CH_4 separation factor was 29.64 when the DEA rate was 16 L/h. The CO_2 flow rate is 10.11×10^{-3} mol m^{-2} s^{-1}, and the CH_4 concentration on the collecting side of the OH/SiO_2/PES membrane may even reach 99.9%. The separation coefficient is as high as 699.54 at the same moment. It is clear that when DEA flow rate and CH_4 concentration rise, the composite membrane's separation effect always outperforms the original membrane's, and the separation factor gap between the composite membranes and the unmodified membranes widens.

The core of the GLMC generated by the GPHM after hydroxylation was chosen for testing to see how the concentration of the absorbent affected the effectiveness of gas separation. The outcomes were displayed in Fig. 13 a and 13 b. Pure PES membrane and composite membrane each experienced an increase in CO_2 flow and CO_2/CH_4 separation factor when the absorbent concentration went from 0.1 mol/L to 2 mol/L. The CO_2 flow and separation factor of the original PES membrane were 9.46×10^{-3} mol m^{-2} s^{-1} and 1.43, respectively, under the condition of DEA concentration of 0.1 mol/L, which were even marginally greater than those of the modified membrane (9.44×10^{-3} mol m^{-2} s^{-1}) and separation factor (1.38). It demonstrated that at a lower absorbent concentration, the membrane alteration has little effect on how well the membrane separates. The reason is that the concentration of DEA is too low, which leads to poor CO_2 mass transfer power. The decisive factor of transmembrane transport is the concentration difference. The hydrophobicity of the membrane material as the interface barrier ignores the viscous effect of the turbulent liquid. The interface thickening after modification will even slightly affect the difficulty of CO_2 transmembrane transport. The CO_2 flux and separation factor of the original membrane rose from 9.87×10^{-3} mol m^{-2} s^{-1} and 5.08 to 9.98×10^{-3} mol m^{-2} s^{-1} and 9.59, respectively, as the concentration of DEA continued to rise from 1.5 mol/L to 2 mol/L. In the OH/SiO_2/PES membrane, the CO_2 flow and separation factor rose from 9.95×10^{-3} mol m^{-2} s^{-1} and 7.88 to 10.04×10^{-3} mol m^{-2} s^{-1} and 20.17, respectively. The separation factor of the composite membrane and the original membrane differs more when the absorbent concentration is higher, suggesting that the membranes' separation performance gap is wider. The effect of material concentration differential as a mass transfer factor is less the higher the DEA concentration. It is no longer important how concentrated the absorbent is on the membrane's cavity and shell sides. By decreasing the viscosity resistance of the liquid at the interface and increasing its hydrophobicity, the membrane's ability to separate particles is further enhanced.

The effect of gas flow rate on membrane separation performance was investigated under the same experimental conditions as the above single factor experiment. As can be observed in Fig. 14 a, as gas flow rate rises, pure PES membrane and OH/SiO_2/PES composite membrane CO_2 concentrations on the gas collecting side increase and the CO_2 flux decreases. The pure PES membrane on the gas collecting side had a CO_2 concentration of 1.2% at a gas flow rate of 30 ml/min, and the associated CO_2 flux was 10.08×10^{-3} mol m^{-2} s^{-1}. The CO_2 flow was 10.11×10^{-3} mol m^{-2} s^{-1}, and the CO_2 content collected by the composite membrane on the gas collecting side was 0.08%. The CO_2 flux of pure PES membrane reduced from 9.59×10^{-3} mol m^{-2} s^{-1} to 9.43×10^{-3} mol m^{-2} s^{-1} when the gas flow rate rose from 120 ml/min to 150 ml/min. Fig. 14 b provides a more comprehensible visual representation of the connection between CH_4 concentration and separation factor on the collecting side. The pure PES membrane collected 98.8% of the CH_4 at the gas collecting side at a gas flow rate of 30 ml/min, and the separation factor could reach 54.89. On the gas collecting side, the composite membrane has a 99.92% CH_4 content collection rate and a high separation factor of 832.67. The original PES membrane's CH_4

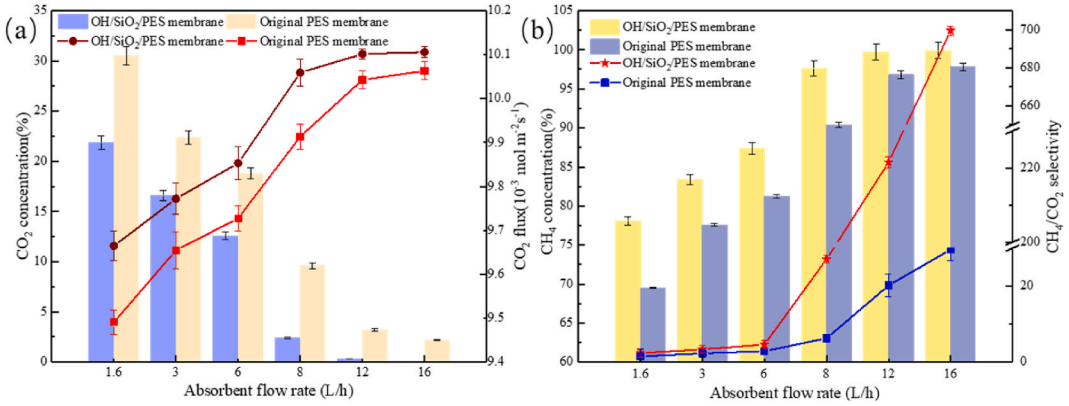

Fig. 12. Effect of absorbent flow rate on gas separation performance of PES composite membrane (a) CO_2 concentration, CO_2 flux (b) CH_4 concentration, CH_4/CO_2 separation factor.

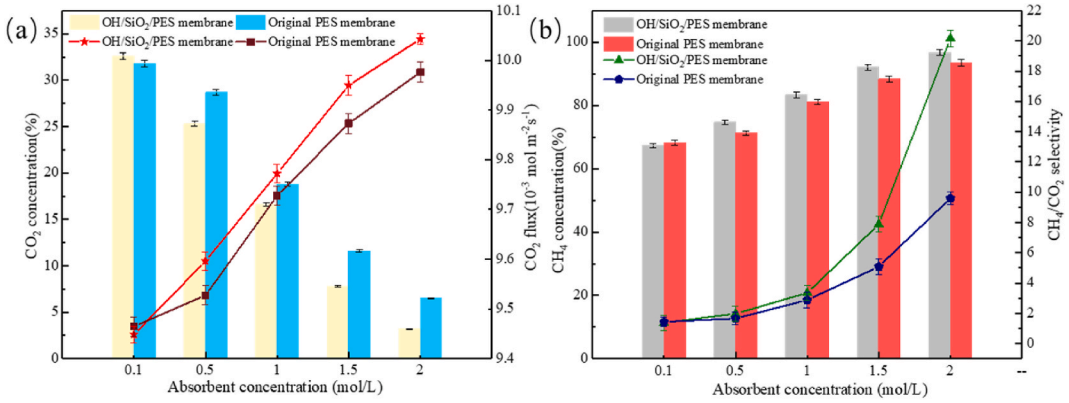

Fig. 13. Effect of absorbent concentration on gas separation performance of PES composite membrane (a) CO_2 concentration, CO_2 permeation flux (b) CH_4 concentration, CH_4/CO_2 separation factor.

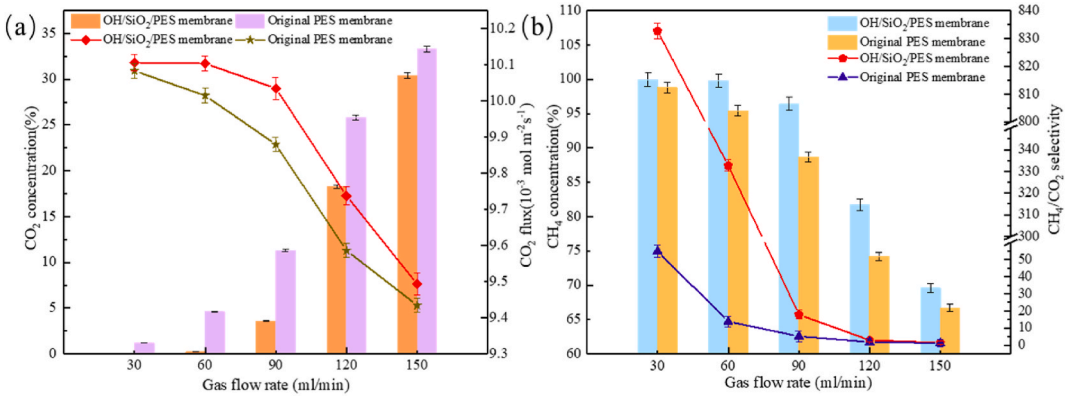

Fig. 14. Effect of gas flow rate on gas separation performance of PES composite membrane. (a) CO_2 concentration, CO_2 permeation flux (b) CH_4 concentration, CH_4/CO_2 separation factor.

concentration dropped from 74.2% to 66.7% and the separation factor from 1.92 to 5.23 with the gas flow rate raised from 120 ml/min to 150 ml/min. The separation factor dropped from 2.98 to 1.34, while the membrane's CH_4 concentration dropped from 81.7% to 69.6%. It has been discovered that the feed gas flow rate significantly affects the membrane's ability to separate gases.

The separation factors of the composite membrane and the original membrane dramatically decrease when the gas flow rate rises, and the gap continues to close, showing that the gas flow rate is the primary determinant of the membrane separation performance.

The reason why CO_2 and CH_4 are separated by GLMC is because CO_2 may react with amine solution whereas CH_4 cannot react with absorbent and has a very poor solubility in amine solution. As a secondary amine, DEA may have its flow rate and concentration increased without affecting the flux of the absorbent. Le Chatelier's principle states that as a result of the rise in reactant concentration, the reaction is carried out in a positive direction and the chemical equilibrium is restored in order to counter the rise in reactant concentration. Increasing the concentration and flow rate of DEA can maximize the right shift of the equilibrium, and CO_2 is fully absorbed. Second, the gas flow rate displays how many moles of gas are produced per unit time. More absorbents are required because more CO_2 has to be absorbed per unit of time as the gas flow rate increases. When the amount of absorbent is constant, when the amount of CO_2 that needs to be absorbed exceeds the absorption limit of DEA, the separation efficiency will be greatly reduced. Since the modified composite membrane we used in GLMC is more hydrophobic than the pure PES membrane, the viscosity between DEA and the membrane is reduced.

In the gas-liquid membrane contactor, although the membrane only as the contact interface between gas and liquid does not have the screening performance, the residence time of the absorbent and the mixture on the membrane surface and the mass transfer resistance become the main factors affecting the CO_2/CH_4 separation performance. The membrane after surface modification is highly hydrophobic. According to the contact angle (CA) theory, when $\theta > 90^\circ$, the solid surface is hydrophobic, and the liquid is not easy to wet the solid and easily moves on the membrane surface. The larger the contact angle is, the closer the liquid is to the shape of the ball on the membrane surface. The larger the contact angle, the more hydrophobic the membrane, so that the viscous resistance between the liquid and the membrane surface is smaller. The decrease of the mass transfer resistance of the absorbent on the liquid side will lead to a decrease in the membrane resistance per unit area per unit time, thereby increasing the separation performance of the membrane.

The separation of CO_2 and CH_4 was more effective thanks to the lower mass transfer barrier between the DEA and the PES. In conclusion, the efficiency of CO_2/CH_4 separation may be significantly increased by increasing absorbent concentration and flow rate and decreasing gas flow rate.

3.2.3. Comparison of the membranes in GLMC with membrane distillation and other membrane reactors

Membrane distillation is a non-isothermal process based on membrane, which is mainly driven by the temperature gradient generated on the membrane. The feed solution on the feed side of the membrane is heated to a temperature below the boiling point. The other side of the membrane is the permeable side, containing cold solution, which may or may not contact with the membrane. When water evaporates from the feed side, it moves through the membrane to the cold permeate side. Water vapor condenses into fresh water after infiltration [48]. Both the gas-liquid membrane contactor and the membrane in membrane distillation act as barriers on the feed side and the permeation side, and do not have a separation effect. There are similarities between the two at this point. However, the membrane in the membrane distillation reactor is not only prone to membrane wetting, but also has low permeation flux. When dealing with water with high salt content or high solute concentration, the solute tends to adhere to the hydrophobic membrane. Moreover, the wastewater on the feed side contains solvents and acids, which greatly reduce the surface tension of the feed solution. This will not only lead to rapid wetting of the membrane, but also cause pollution, resulting in membrane damage and increasing the capital cost of replacing the membrane [49]. In addition, various pollutants can accelerate membrane wetting while reducing flux. Our modified OH/SiO_2/PES composite membrane successfully avoided the above problems in the separation of CO_2/CH_4 mixture in GLMC.

The better performance of the gas-liquid membrane contactor is due to the reduced wettability of the membrane [50]. The liquid on the membrane surface is close to spherical, which confirms that the hydrophobic properties of the membrane can be improved by the application of modification technology, which can reduce the viscous resistance between the liquid and the membrane surface. The greater the hydrophobicity of the membrane, the smaller the degree of membrane wetting [51]. The liquid on the surface of the membrane is nearly spherical, which indicates that the hydrophobicity of the membrane increases. The increase in hydrophobicity leads to a decrease in the wettability of the membrane, which makes the gas-liquid membrane contactor have better separation performance [52].

Compared with other membrane contactors [53,54], our modified OH/SiO_2/PES composite membrane has better separation effect on CO_2/CH_4 mixture in GLMC. Favre, E used membrane contactors to absorb post-combustion carbon dioxide into chemical solvents and applied it to the latest status of operating conditions and process performance of packed towers for CO_2 capture [54]. Abu Hatab, F et al. introduced glass beads on the shell side of the membrane contactor. The results show that the CO_2 removal efficiency is increased by 21% when the shell is filled with glass beads [53]. In this paper, the OH/SiO_2/PES composite membrane prepared has a separation factor of 833.67 for CO_2/CH_4 and can separate CH_4 with a purity of more than 99.9%, where separation effect is far more than other membrane contactors.

From the grafting rate, the SiO_2 grafting rate of the composite membrane prepared by the gas phase hydrolysis method is not much different from that of the grafting coating method. From the perspective of the uniformity of grafted inorganic particles, the surface particles of the composite membrane prepared by the gas phase hydrolysis method are more uniform than those prepared by the grafting coating method. From the analysis of chemical bonds, the chemical bond peak of the SiO_2 crystal formed by the composite membrane prepared by the gas phase hydrolysis method is higher than that of the composite membrane prepared by the grafting coating method, indicating that the grafting amount on the surface of the composite membrane prepared by the gas phase hydrolysis method is larger. It can be directly observed from the gas separation performance experiment that the PES composite membrane prepared by gas phase hydrolysis after alkali treatment has the best separation effect on CO_2/CH_4 in the gas-liquid membrane contactor. The above analysis shows that the gas phase hydrolysis method can also successfully modify the surface of the PES membrane, and the modification effect is better than that of the PES composite membrane prepared by the grafting coating method.

4. Conclusions

In this study, OH/SiO_2/PES membranes were prepared for the separation of CO_2/CH_4 in GLMC. Using different characterizations, the modified membranes made by the GPHM and the GCM were compared. Also, the impact of hydroxylation on the preparation technique was assessed. The effective grafting of SiO_2 enhanced the interface's hydrophobicity and mechanical characteristics, according to characterization. When we tested the CO_2/CH_4 separation coefficient, we discovered that the modified membrane had a higher capacity to trap CO_2 than the original PES membrane, which improved the CO_2/CH_4 separation effect. After separating the combined gas at a rate of 30 ml per minute, CH_4 concentration was 99.92%. The separation coefficient was 833.67 and the CO_2 flow was 10.1059×10^{-3} mol m^{-2} s^{-1}. This paper presents a novel CO_2/CH_4 separation technique in GLMC employing fluorinated OH/SiO_2/PES membranes. In the future, modified PES composite membranes could offer a fresh approach to CO_2/CH_4 separation. It is expected that the developed technologies can be extended to other applications with a combination of CO_2 recycling methods [55].

Author contribution statement

Zhengda Lin: Conceived and designed the experiments; Performed the experiments; Analyzed and interpreted the data; Contributed reagents, materials, analysis tools or data; Wrote the paper.

Dandan Zhang; Rui Wu; Rui Fang: Analyzed and interpreted the data.

Yijun Liu; Zhongming Zhang: Performed the experiments.

Zhiying Zhao; Bo Shao; Jie Yao: Contributed reagents, materials, analysis tools or data.

Data availability statement

Data will be made available on request.

Declaration of competing interest

The authors declare that they have no known competing financial interests or personal relationships that could have appeared to influence the work reported in this paper.

Acknowledgments

This work was supported by Preparation of Organic - inorganic Hybrid Membrane and Study on Its Oil and Phenol Removal Process [grant number MH20220979].

References

[1] E.M. Arrieta, M. Geri, J.B. Coquet, C.M. Scavuzzo, M.E. Zapata, A.D. Gonzalez, Quality and environmental footprints of diets by socio-economic status in Argentina, Sci, Total Environ. 801 (2021) 10, https://doi.org/10.1016/j.scitotenv.2021.149686.

[2] T.K.L. Nguyen, H.H. Ngo, W.S. Guo, L.D. Nghiem, G.R. Qian, Q. Liu, J.Y. Liu, Z. Chen, X.T. Bui, B. Mainali, Assessing the environmental impacts and greenhouse gas emissions from the common municipal wastewater treatment systems, Sci. Total Environ. 801 (2021) 9, https://doi.org/10.1016/j.scitotenv.2021.149676.

[3] C.Y. Chuah, S. Anwar, P. Weerachanchai, T.H. Bae, K. Goh, R. Wang, Scaling-up defect-free asymmetric hollow fiber membranes to produce oxygen-enriched gas for integration into municipal solid waste gasification process, J. Membr. Sci. 640 (2021) 10, https://doi.org/10.1016/j.memsci.2021.119787.

[4] C. Zhou, X. Liu, Y. Zhao, X. Yang, Y. Li, L. Dong, C. Duan, Z. Rao, Recent progress and potential challenges in coal upgrading via gravity dry separation technologies, Fuel 305 (2021), https://doi.org/10.1016/j.fuel.2021.121430.

[5] A.A. Abd, M.R. Othman, Biogas upgrading to fuel grade methane using pressure swing adsorption: parametric sensitivity analysis on an industrial scale, Fuel 308 (2022) 11, https://doi.org/10.1016/j.fuel.2021.121986.

[6] X.Z. He, L.F. Lei, Z.D. Dai, Green hydrogen enrichment with carbon membrane processes: techno-economic feasibility and sensitivity analysis, Sep. Purif. Technol. 276 (2021) 9, https://doi.org/10.1016/j.seppur.2021.119346.

[7] M. Balcik, S.B. Tantekin-Ersolmaz, I. Pinnau, M.G. Ahunbay, CO2/CH4 mixed-gas separation in PIM-1 at high pressures: bridging atomistic simulations with process modeling, J. Membr. Sci. 640 (2021) 12, https://doi.org/10.1016/j.memsci.2021.119838.

[8] X. Lv, L. Huang, S.Y. Ding, J.N. Wang, L. Li, C. Liang, X.Q. Li, Mixed matrix membranes comprising dual-facilitated bio-inspired filler for enhancing CO2 separation, Sep. Purif. Technol. 276 (2021) 11, https://doi.org/10.1016/j.seppur.2021.119347.

[9] M.A. Guseva, D.A. Alentiev, D.S. Bakhtin, I.L. Borisov, R.S. Borisov, A.V. Volkov, E.S. Finkelshtein, M.V. Bermeshev, Polymers based on exo-silicon-substituted norbornenes for membrane gas separation, J. Membr. Sci. 638 (2021) 15, https://doi.org/10.1016/j.memsci.2021.119656.

[10] C.-D. Ho, H. Chang, Y.-H. Chen, J.-W. Lim, J.-W. Liou, Conjugated mass transfer of CO2 absorption through concentric circular gas-liquid membrane contactors, Processes 9 (9) (2021), https://doi.org/10.3390/pr9091580.

[11] Q.P. Xin, X. Li, H.L. Hou, Q.Q. Liang, J.P. Guo, S.F. Wang, L. Zhang, L.G. Lin, H. Ye, Y.Z. Zhang, Superhydrophobic surface-constructed membrane contactor with hierarchical lotus-leaf-like interfaces for efficient SO2 capture, ACS Appl. Mater. Interfaces 13 (1) (2021) 1827–1837, https://doi.org/10.1021/acsami.0c17534.

[12] S.R. Chavan, P. Perre, V. Pozzobon, J. Lemaire, CO2 absorption using hollow fiber membrane contactors: introducing pH swing absorption (pHSA) to overcome purity limitation, Membranes 11 (7) (2021) 18, https://doi.org/10.3390/membranes11070496.

[13] Y.L. Xu, X. Li, Y.Q. Lin, C. Malde, R. Wang, Synthesis of ZIF-8 based composite hollow fiber membrane with a dense skin layer for facilitated biogas upgrading in gas-liquid membrane contactor, J. Membr. Sci. 585 (2019) 238–252, https://doi.org/10.1016/j.memsci.2019.05.042.

[14] Y.L. Xu, Y.Q. Lin, N.G.P. Chew, C. Malde, R. Wang, Biocatalytic PVDF composite hollow fiber membranes for CO2 removal in gas-liquid membrane contactor, J. Membr. Sci. 572 (2019) 532–544, https://doi.org/10.1016/j.memsci.2018.11.043.

[15] Y.L. Xu, Y.Q. Lin, M. Lee, C. Malde, R. Wang, Development of low mass-transfer-resistance fluorinated TiO2-SiO2/PVDF composite hollow fiber membrane used for biogas upgrading in gas-liquid membrane contactor, J. Membr. Sci. 552 (2018) 253–264, https://doi.org/10.1016/j.memsci.2018.02.016.

[16] N.A. Ahmad, C.P. Leo, A.L. Ahmad, M.N. Izwanne, Swelling reduction of polyvinylidenefluoride hollow fiber membrane incorporated with silicoaluminophosphate-34 zeotype filler for membrane gas absorption, Sep. Purif. Technol. 212 (2019) 941–951, https://doi.org/10.1016/j.seppur.2018.12.015.
[17] P. Xu, Y. Huang, X.L. Kong, D.W. Gong, K.Y. Fu, X.F. Chen, M.H. Qiu, Y.Q. Fan, Hydrophilic membrane contactor for improving selective removal of SO2 by NaOH solution, Sep. Purif. Technol. 250 (2020) 9, https://doi.org/10.1016/j.seppur.2020.117134.
[18] M. Chai, A. Razmjou, V. Chen, Metal-organic-framework protected multi-enzyme thin-film for the cascade reduction of CO2 in a gas-liquid membrane contactor, J. Membr. Sci. 623 (2021) 11, https://doi.org/10.1016/j.memsci.2020.118986.
[19] F. Shabani, M.A. Aroon, T. Matsuura, R. Farhadi, CO2/CH4 separation properties of PES mixed matrix membranes containing Fullerene-MWCNTs hybrids, Sep. Purif. Technol. 277 (2021) 13, https://doi.org/10.1016/j.seppur.2021.119636.
[20] A. Rosli, A.L. Ahmad, S.C. Low, Enhancing membrane hydrophobicity using silica end-capped with organosilicon for CO2 absorption in membrane contactor, Sep. Purif. Technol. 251 (2020) 11, https://doi.org/10.1016/j.seppur.2020.117429.
[21] S. Shirazian, A.T. Nakhjiri, A. Heydarinasab, M. Ghadiri, Theoretical investigations on the effect of absorbent type on carbon dioxide capture in hollow-fiber membrane contactors, PLoS One 15 (7) (2020) 15, https://doi.org/10.1371/journal.pone.0236367.
[22] X.N. Wu, B. Zhao, L. Wang, Z.H. Zhang, M. Li, Preparation and characterization of superhydrophobic PVDF/HMSNs hybrid membrane for CO2 absorption, Polymer 214 (2021) 10, https://doi.org/10.1016/j.polymer.2020.123242.
[23] A. Talauari, B. Ghanauati, A. Azimi, S. Sayyahi, Preparation and characterization of PVDF-filled MWCNT hollow fiber mixed matrix membranes for gas absorption by Al2O3 nanofluid absorbent via gas-liquid membrane contactor, Chem. Eng. Res. Des. 156 (2020) 478–494, https://doi.org/10.1016/j.cherd.2020.01.017.
[24] S.A. Hashemifard, M.S. Ghodrati, M. Rezaei, A.A. Izadpanah, Experimental study of gas dehydration via PDMS/CaCO3 NP-coated PVC hollow fiber membrane contactor, Chem. Eng. Res. Des. 162 (2020) 62–73, https://doi.org/10.1016/j.cherd.2020.07.032.
[25] S.M. Mirfendereski, Z. Niazi, T. Mohammadi, Selective removal of H2S from gas streams with high CO2 concentration using hollow-fiber membrane contractors, Chem. Eng. Technol. 42 (1) (2019) 196–208, https://doi.org/10.1002/ceat.201800014.
[26] M. Baniamer, A. Aroujalian, S. Sharifnia, A novel PEBAX-1657/PES-(BiFeO3@ZnS) photocatalytic membrane for integrated hybrid systems coupling CO2 separation and photoreduction, J. Environ. Chem. Eng. 9 (6) (2021) 12, https://doi.org/10.1016/j.jece.2021.106529.
[27] S. Ghorabi, F.Z. Ashtiani, M. Karimi, A. Fouladitajar, B. Yousefi, F. Dorkalam, Development of a novel dual-bioinspired method for synthesis of a hydrophobic/hydrophilic polyethersulfone coated membrane for membrane distillation, Desalination 517 (2021) 17, https://doi.org/10.1016/j.desal.2021.115242.
[28] C.Y. Tong, Y.S. Chang, B.S. Ooi, D.J.C. Chan, Physico-chemistry and adhesion kinetics of algal biofilm on polyethersulfone (PES) membrane with different surface wettability, J. Environ. Chem. Eng. 9 (6) (2021), https://doi.org/10.1016/j.jece.2021.106531.
[29] A. Suhaimi, E. Mahmoudi, R. Latif, K.S. Siow, M.H.M. Zaid, A.W. Mohammad, M.F.M.R. Wee, Superhydrophilic organosilicon plasma modification on PES membrane for organic dyes filtration, J. Water Process Eng. 44 (2021), https://doi.org/10.1016/j.jwpe.2021.102352.
[30] C.M. Gao, H.Y. Chen, S.H. Liu, Y.Q. Xing, S.F. Ji, J.C. Chen, J.J. Chen, P. Zou, J.N. Cai, Preparing hydrophilic and antifouling polyethersulfone membrane with metal-polyphenol networks based on reverse thermally induced phase separation method, Surface. Interfac. 25 (2021) 13, https://doi.org/10.1016/j.surfin.2021.101301.
[31] H.L. Pang, Z.Z. Chen, H.J. Gong, M.F. Du, Fabrication of a super hydrophobic polyvinylidene fluoride-hexadecyltrimethoxysilane hybrid membrane for carbon dioxide absorption in a membrane contactor, J. Membr. Sci. 595 (2020) 10, https://doi.org/10.1016/j.memsci.2019.117536.
[32] N. Akhlaghi, G. Najafpour-Darzi, M. Mohammadi, Surface modification of magnetic MnFe2O4@SiO2 core-shell nanoparticles with deposited layer of 3-aminopropyl triethoxysilane, Iran, J. Mater. Sci. Eng. 17 (4) (2020) 77–86, https://doi.org/10.22068/ijmse.17.4.8.
[33] O. Johnson, B. Joseph, J.N. Kuhn, CO2 separation from biogas using PEI-modified crosslinked polymethacrylate resin sorbent, J. Ind. Eng. Chem. 103 (2021) 255–263, https://doi.org/10.1016/j.jiec.2021.07.038.
[34] J. Ghobadi, D. Ramirez, S. Khoramfar, R. Jerman, M. Crane, K. Hobbs, Simultaneous absorption of carbon dioxide and nitrogen dioxide from simulated flue gas stream using gas-liquid membrane contacting system, Int. J. Greenh. Gas Control 77 (2018) 37–45, https://doi.org/10.1016/j.ijggc.2018.07.026.
[35] B. Liu, D. Li, J. Yao, H. Sun, Improved CO2 separation performance and interfacial affinity of mixed matrix membrane by incorporating UiO-66-PEI@ bmim Tf2N particles, Sep. Purif. Technol. 239 (2020) 11, https://doi.org/10.1016/j.seppur.2020.116519.
[36] Y. Berbar, Z.E. Hammache, S. Bensaadi, R. Soukeur, M. Amara, B. Van der Bruggen, Effect of functionalized silica nanoparticles on sulfonated polyethersulfone ion exchange membrane for removal of lead and cadmium ions from aqueous solutions, J. Water Process Eng. 32 (2019) 7, https://doi.org/10.1016/j.jwpe.2019.100953.
[37] M. Shakak, R. Rezaee, A. Maleki, A. Jafari, M. Safari, B. Shahmoradi, H. Daraei, S.M. Lee, Synthesis and characterization of nanocomposite ultrafiltration membrane (PSF/INP/SiO2) and performance evaluation for the removal of amoxicillin from aqueous solutions, Environ. Technol. Innov. 17 (2020) 14, https://doi.org/10.1016/j.eti.2019.100529.
[38] S. Khodadousti, F.Z. Ashtiani, M. Karimi, A. Fouladitajar, Preparation and characterization of novel PES-(SiO2-g-PMAA) membranes with antifouling and hydrophilic properties for separation of oil-in-water emulsions, Polym. Adv. Technol. 30 (9) (2019) 2221–2232, https://doi.org/10.1002/pat.4651.
[39] B. Jaleh, E. Zare, S. Azizian, O. Qanati, M. Nasrollahzadeh, R.S. Varma, Preparation and characterization of polyvinylpyrrolidone/polysulfone ultrafiltration membrane modified by graphene oxide and titanium dioxide for enhancing hydrophilicity and antifouling properties, J. Inorg. Organomet. Polym. Mater. 30 (6) (2020) 2213–2223, https://doi.org/10.1007/s10904-019-01367-x.
[40] T. Barzegar, S. Hassanajili, Fabrication and characterization of dual layer PEBAX-SiO2/polyethersulfone nanocomposite membranes for separation of CO2/CH4 gases, J. Appl. Polym. Sci. 139 (6) (2022) 18, https://doi.org/10.1002/app.51624.
[41] S. Kamari, A. Shahbazi, Biocompatible Fe3O4@SiO2-NH2 nanocomposite as a green nanofiller embedded in PES-nanofiltration membrane matrix for salts, heavy metal ion and dye removal: long-term operation and reusability tests, Chemosphere 243 (2020) 13, https://doi.org/10.1016/j.chemosphere.2019.125282.
[42] Y. Kourde-Hanafi, P. Loulergue, A. Szymczyk, B. Van der Bruggen, M. Nachtnebel, M. Rabiller-Baudry, J.L. Audic, P. Polt, K. Baddari, Influence of PVP content on degradation of PES/PVP membranes: insights from characterization of membranes with controlled composition, J. Membr. Sci. 533 (2017) 261–269, https://doi.org/10.1016/j.memsci.2017.03.050.
[43] P. Amirabedi, A. Akbari, R. Yegani, Fabrication of hydrophobic PP/CH3SiO2 composite hollow fiber membrane for membrane contactor application, Sep. Purif. Technol. 228 (2019) 10, https://doi.org/10.1016/j.seppur.2019.115689.
[44] S. Acarer, I. Pir, M. Tufekci, G.T. Demirkol, N. Tufekci, Manufacturing and characterisation of polymeric membranes for water treatment and numerical investigation of mechanics of nanocomposite membranes, Polymers 13 (10) (2021) 23, https://doi.org/10.3390/polym13101661.
[45] Y.N. Li, Y.C. Hao, H. Ye, Y.Z. Zhang, Y. Chen, X.J. Xu, Single-sided superhydrophobic fluorinated silica/poly(ether sulfone) membrane for SO2 absorption, J. Membr. Sci. 580 (2019) 190–201, https://doi.org/10.1016/j.memsci.2019.03.016.
[46] H.X. Yu, X.F. Zhang, Y.T. Zhang, J.D. Liu, H.Q. Zhang, Development of a hydrophilic PES ultrafiltration membrane containing SiO2@N-Halamine nanoparticles with both organic antifouling and antibacterial properties, Desalination 326 (2013) 69–76, https://doi.org/10.1016/j.desal.2013.07.018.
[47] H. Zhang, K.L. Xue, C. Cheng, D. Gao, H.P. Chen, Study on the performance of CO2 capture from flue gas with ceramic membrane contactor, Sep. Purif. Technol. 265 (2021) 9.
[48] M. Qasim, I. Ul Samad, N.A. Darwish, N. Hilal, Comprehensive review of membrane design and synthesis for membrane distillation, Desalination 518 (2021) 65, https://doi.org/10.1016/j.desal.2021.115168.
[49] M. Afsari, H.K. Shon, L.D. Tijing, Janus membranes for membrane distillation: recent advances and challenges, Adv. Colloid Interface Sci. 289 (2021) 22, https://doi.org/10.1016/j.cis.2021.102362.
[50] Y. Li, R.N. Gao, J.W. Zhang, Y. Zhang, S. Liang, Antifouling conductive composite membrane with reversible wettability for wastewater treatment, Membranes 12 (6) (2022) 11, https://doi.org/10.3390/membranes12060626.

[51] L.B. Zheng, M. Tang, Y.Z. Wang, D.Y. Hou, X.Y. Li, J. Wang, A novel Cu-BTC@PVA/PVDF Janus membrane with underwater-oleophobic/hydrophobic asymmetric wettability for anti-fouling membrane distillation, Sep. Purif. Technol. 299 (2022) 11, https://doi.org/10.1016/j.seppur.2022.121807.
[52] H.Q. Chang, B.C. Liu, Z.W. Zhang, R. Pawar, Z.S. Yan, J.C. Crittenden, R.D. Vidic, A critical review of membrane wettability in membrane distillation from the perspective of interfacial interactions, Environ. Sci. Technol. 55 (3) (2021) 1395–1418, https://doi.org/10.1021/acs.est.0c05454.
[53] F. Abu Hatab, N. Abdullatif, S.A.M. Marzouk, M.H. Al-Marzouqi, Experimental and modeling of CO2 removal from gas mixtures using membrane contactors packed with glass beads, Sep. Purif. Technol. 217 (2019) 240–246, https://doi.org/10.1016/j.seppur.2019.01.081.
[54] E. Favre, H.F. Svendsen, Membrane contactors for intensified post-combustion carbon dioxide capture by gas-liquid absorption processes, J. Membr. Sci. 407 (2012) 1–7, https://doi.org/10.1016/j.memsci.2012.03.019.
[55] M. Visnyei, P. Bakonyi, K. Belafi-Bako, N. Nemestothy, Integration of gas-liquid membrane contactors into anaerobic digestion as a promising route to reduce uncontrolled greenhouse gas (CH(4)/CO(2)) emissions, Bioresour. Technol. 364 (2022), 128072, https://doi.org/10.1016/j.biortech.2022.128072.